DEVELOPMENT OF A NOVEL ELECTROCARDIOGRAPHY SENSOR BASED ON A COMPOSITE SILVER CHLORIDE NANOPARTICLES AND POLYANILINE

A Thesis Submitted to
the Graduate School of Engineering and Sciences of
İzmir Institute of Technology
in Partial Fulfillment of the Requirements for the Degree of

MASTER OF SCIENCE
in Chemistry

by
Didem TAŞCIOĞLU

June 2013

We approve the thesis of **Didem TAŞCIOĞLU**

Examining Committee Members:

_____
Prof. Dr. Serdar ÖZÇELİK
Department of Chemistry, İzmir Institute of Technology

_____
Assoc. Prof. Dr. Mustafa M. DEMİR
Department of Chemistry, İzmir Institute of Technology

_____
Prof. Dr. Suna TİMUR
Department of Biochemistry, Ege University

6 June 2013

_____
Prof. Dr. Serdar ÖZÇELİK
Supervisor, Department of Chemistry
İzmir Institute of Technology

_____   _____
Prof. Dr. Durmuş ÖZDEMİR   **Prof. Dr. R. Tuğrul SENGER**
Head of the Department of Chemistry   Dean of the Graduate School of
                                         Engineering and Sciences

ACKNOWLEDGEMENTS

ABSTRACT

DEVELOPMENT OF A NOVEL ELECTROCARDIOGRAPHY SENSOR BASED ON A COMPOSITE SILVER CHLORIDE NANOPARTICLES AND POLYANILINE

The electrical activity of the heart is detected by electrodes attached to the surface of the skin. These electrodes detect bioelectrical signals in the human body. Physilogical status of heart condition especially cardiovascular diseases and disturbances in the cardiac rthym are recorded by electrocardiography (ECG). Despite the fact that the usage of disposable ECG electrodes in our country is substantial nearly as 70 million in 2010, these electrodes are not fabricated in Turkey. In the scope of this study, it was aimed to develop a novel sensor based on synthesized AgCl/Polyaniline nanocomposites for ECG electrodes.

In this study, the production of silver chloride (AgCl) nanoparticles was achieved by the polyol method. ABS (Acrylonitrile butadiene styrene) was used as a supporting material of the ECG electrode. Synthesized AgCl nanoparticles were not easily adsorbed on the surface of ABS. We develop a synthetic chemistry to perform simultaneous synthesis of AgCl nanoparticle and polymerization of aniline on surface of ABS. Polyaniline acts as a chemical linker between the nanoparticle and ABS surface in the same batch reactor. The synthesized composite based on polyaniline and AgCl nanoparticles completely covers the surface of ABS.

To evaluate electrodes, we fabricated a disposable ECG electrode and compared it with the disposable electrodes that are commercially available. The electrocardiography data indicated that the fabricated electrodes were demonstrated a performance which is comparable with the commercial electrodes. The results demonstrate that a novel ECG electrodes can be manufactured based on this new composite material and method develop in our laboratory.

ÖZET

GÜMÜŞ KLORÜR NANOTANECİKLER VE POLİANİLİN İÇEREN KOMPOZİT ESASLI YENİ BİR ELEKTROKARDİYOGRAFİ SENSÖRÜNÜN GELİŞTİRİLMESİ

Kalbin elektriksel aktivitesi derinin yüzeyine bağlanmış elektrotlar ile tespit edilir. Bu elektrotlar sayesinde vücuttaki elektriksel kökenli biyolojik işaretler algılanarak kalp damar hastalıkları ve ileti bozuklukları başta olmak üzere çeşitli kalp rahatsızlıkları elektrokardiyografi (ECG) tarafından kaydedilir. EKG elektrotlarının ülkemizde kullanımı çok yüksek miktarda (2010 yılında yaklaşık 70 milyon) olmasına rağmen, bu elektrotlardaki sensörlerin yerli üretimi yapılmamaktadır. Bu çalışma kapsamında EKG elektrotları için gümüş klorür/polyaniline (AgCl/PANI) nanokompozit malzemeye dayalı yeni bir sensörün geliştirilmesi amaçlanmıştır.

Bu çalışmada, gümüş klorür (AgCI) nanotaneciklerin sentezi poliol yöntem ile yapılmıştır. Ancak, AgCI nanotaneciklerin EKG elektrodunun destek malzemesi olan ABS yüzeyine kaplanması zor olmaktadır. Bu nedenle, nanotanecik ile ABS arasında kimyasal bağlayıcı görevi görmesi için iletken bir polimer olan polianilin seçilmiştir. Polianilin sentezi ile AgCl nanotanecik sentezi aynı anda ve aynı ortamda yapılmıştır. Böylece polianilin içerindeki AgCl nanotaneciklerin ABS yüzeyine bağlanması sağlanmıştır.

Laboratuvarımızda geliştirdiğimiz kompozit malzemeye dayalı sensörlerden yapılan tek kullanımlık elektrotlar ile ticari elektrotların performansları karşılaştırılmıştır. Geliştirilen elektrotlar ile elde edilen elektrokardiyografi verilerinin ticari olarak kullanılan elektrotlar ile karşılaştırılabilir veya daha iyi sinyal/gürültü oranına sahip olduğu belirlenmiştir. Bu sonuçlar, geliştirilen malzeme ve üretim yöntemi ile EKG elektrotlarının ülkemizde imal edileceğini göstermektedir.

TABLE OF CONTENTS

LIST OF FIGURES

LIST OF TABLES

CHAPTER 1

INTRODUCTION

1.1.   Nanotechnology and Metal Nanostructures

In 1959, Nobel prize winner, physicist Richard Feynman suggested that a new field about technology at an atomic and molecular scale for science. Richard Feynman, expressed the idea of direction and control everything on a small scale in the name of "There is Plenty of Room at the Bottom" speech, thus nanotechnology came into our life (Blackman 2008). Today, nanotechnology has become a popular field for research and development. The promise and essence of nanotechnology is the ability to work at the molecular level, atom by atom, to create functional materials on the 1 to 100 nanometer (one billionth of a meter) length scale (Ali Mansoori 2005). Nanotechnology demonstrated that physical and chemical properties of nanoscale materials such as electrical conductivity, color, resistance and reactivity etc. behave differently than the large scale materials.

Nanoscience provides that an understanding of new behaviour which is the resulting measures of nanometers with the help of the quantum theory. In case, nanotechnology aimed to design and synthesize nanostructure or to gain new extraordinary features and to use these features at the new functions. In other words, nanotechnology makes known molecules functional by adding new atoms and molecules or synthesizes quantum points and wires. In this way, synthesized structure can be a very active and exhibit extraordinary electronic or magnetic properties. Nanotechnology is compared to all known technologies need a lot more basic science and theoretical research (Ramsden 2009).

In nanotechnology, nanoparticle is defined as a one dimensional object that is a 100 nm or less than 100 nm. Nanoparticles have unique properties because they have large surface area and large surface energy. Nanoparticles show that fascinating optical and electronic properties depends on the size and shape of the particle. The size and the shape of the nanoparticles are controlled by the temperature, stabilizers, pH of the solution, concentration of the reagents and etc. (Wiley et al. 2005). Nanoparticles have a

variety of applications such as optical, electronic, magnetic, biological, catalytic, and biomedical materials, etc. (Coskun, Aksoy, and Unalan 2011).

Noble metal nanoparticles are very important because they have unique physical and chemical properties. Also, metal nanoparticles have important role due to their potential applications. First metal nanoparticle which was synthesized by reduction of gold ion with sodium citrate by J. Turkovich in 1951 was 20 nm gold nanoparticle (Turkevich 1951). This method is still widely used today. The physical, chemical, optical and electronic properties of metal nanoparticles could be controlled by changing size, shape and morphology of these particles (Wiley et al. 2004b). There are different shape particles such as nanorods, nanowires, nanodisks, nanoprisms, etc. due to the effect on the properties of the shape of the particle. A large number of methods have been developed for the synthesis of different shape metal nanoparticles. The most widely used of these methods are such as reduction of metal salt, polyols, the sol-gel, micro-emulsions, etc. (Coskun, Aksoy, and Unalan 2011, Wang et al. 2005). For instance firstly, electrochemical reduction of $HAuCl_4$ was attempted for the synthesis of the Au nanorod. However, in this method, the micellar system consists of two cationic surfactants which are cetyltrimethylammonium bromide (CTAB) and the much more hydrophobic tetradecylammonium bromide (TDAB) or tetraoctylammonium bromide (TOAB), so shape control is very difficult in the electrochemical method (Schonenberger et al. 1997, Martin 1994). Afterwards, the excellent aspect ratio of Au and Ag nanorods were able to synthesize by using Murphy and coworkers methods (Murphy and Jana 2002). In this method the formation of nanorod provided by means of adding a mild reducing agent (ascorbic acid) on the pre-synthesized Au and Ag seeds, in the presence of capping agent (CTAB). The different aspect ratios of Au nanorods could be synthesized with addition of different volumes of the seed solution. Then, this method has been improved by El-Sayed and coworkers, thus the rod yield increased (Nikoobakht and El-Sayed 2003).

Metal nanoparticles are very important and interesting because of the potential application areas. In the last 20 years through the control of morphology during synthesis, studies on the properties and application areas due to morphology have gained momentum. Sanders et al. showed that high-aspect-ratio metal nanostructures, such as Au and Ag nanorods/nanowires, can be used to transport optical signals over distances of several micrometers (Sanders et al. 2006). Due to the optical properties of gold nanorods which are easily conjugated to antibodies or proteins, biocompatible are

promising for photothermal applications (Jain et al. 2006). Also, having the different crystallographic properties of nonspherical particles thanks to the number of corners and faces can be used as a catalyst in fuel cells, waste reduction and the chemical industry (Herron and Thorn 1998). Pal said that known antibacterial property of silver has changed depending on the shape of the silver nanoparticle. According to this study, truncated silver nanotriangles showed more anti-bacterial properties than spherical and rod nanoparticle (Pal, Tak, and Song 2007) . Briefly, we can say that the effect of the shape of metal nanoparticles having the many application areas (microelectronics (Nepijko et al. 2011), sensors (Lee and El-Sayed 2006, Doria et al. 2012), catalysis (Cao, Lu, and Veser 2010), non-linear optical materials (Collier et al. 1997) is very large on application areas.

1.2. Wet Chemical Methods for the Preparation of Colloidal Metal Nanoparticle

Several methods have been developed for synthesis of metal nanoparticles such as chemical reduction of metal salts, microemulsion method, sonochemical reduction and electrochemical synthesis (Cushing, Kolesnichenko, and O'Connor 2004).

These are very important to prepare ideally metal nanoparticles: A method should

> ➢ be reproducible
> ➢ control the shape of the particle
> ➢ be easy and cheap
> ➢ yield monodisperse nanoparticles
> ➢ use the less number of reagents
> ➢ have a few step for synthesis nanoparticle

Chemical reduction of metal salts method is based on the reduction of metal ions with a strong reducing reagent ($NaBH_4$, $N_2H_4.H_2O$, etc.) to metallic particles. Reduction can be performed in media containing both aqueous and organic solvent. The reaction can be occured by the inclusion of reagents, which will be exposed to oxidation and reduction, to the solution and at the end of the reaction, media becomes supersaturated solution with products. Excessive saturation state, the chemical system remove from the

lowest free energy configuration. In the system, thermodynamic equilibrium occurs with the condensation of nucleous and the reaction product creates particles. The last states of the particles reach as a result of nucleation and growth of subsequently developing particles. Figure 1.1 indicates the formation of nanostructured metal colloids.

Nucleation occurs with two ways as homogeneous or heterogeneous. In salt reduction method, rate of reaction and formation of particles are affected from the concentration of reagents, temperature, pH, general structure of mixture and the order of adding reagents.
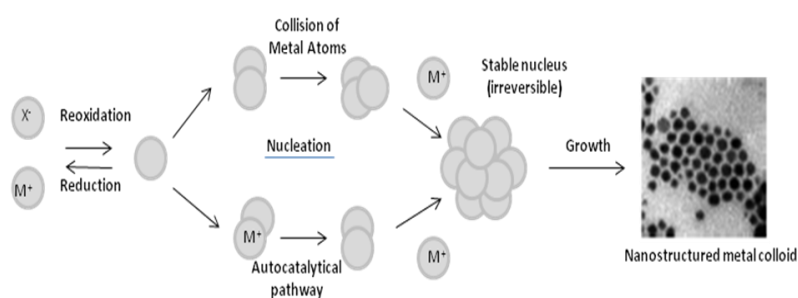
Figure 1.1. Formation of nanostructured metal colloids by the ''salt reduction'' method
(Source: Tang et al. 2009)

This method is one of the mostly used method as seen in the literature. For example, Guzman and coworkers synthesized silver nanoparticle by chemical reduction method to research antibacterial activity of this nanoparticle in 2009 (Maribel G. Guzmán 2009). In this study, they used hydrazine hydrate as a reducing agent. As a result the size of their synthesized nanoparticles is 60 nm. Also, Dang and coworkers prepared copper nanoparticle by using this method (Thi My Dung Dang 2011). Here, they used sodium borohydride as a reducing agent. $NaBH_4$ is a strong reducing agent so the size of the nanoparticles is smaller than the previous example. Size of the synthesized nanoparticles is 10 nm.

Two phase method is easy-performing and show low toxicity. Firstly, Brust and coworkers developed two phase method for the synthesis of Au nanoparticles (M. Brust 1995, M. Brust 1994). In this study, firstly, $HAuCl_4$ is dissolved in water and then it transported into toluene by means of tetraoctylammonium bromide (TOAB), which acts as a phase transfer agent. Transported Au ions are mixed with $NaBH_4$ which is strong

4

reductant, in the presence of capping agent (thioalkanes or aminoalkanes). The particle size can be controlled between ~1 nm and ~10 nm depending on the ratio of the Au salt and capping agent. Kang and coworkers (S. Y. Kang 1998) also used the similar method of two-phase synthesis for Ag nanoparticles..

Another important method was developed by Michel Figlarz in 1983 had implemented the production of metallic nanoparticles by using microwave heating. This method is polyol method. Figure 1.2 shows that experimental setup of the polyol method. The polyol process is based on the reduction of metal salt by ethylene glycol at an elevated temperature. The polyol method requires a metal salt and a reducing agent. In this process, ethylene glycol is used as a reducing agent and solvent. Here, Polyvinyl pyrolidone (PVP) is used as a stabilizer to prevent agglomeration (Ducampsanguesa, Herreraurbina, and Figlarz 1992, Silvert et al. 1996). Also, gelatin, polyvinyl alcohol and polyacrylic acid can be used as a stabilizer in this process. The morphology of metal nanomaterials can be easily controlled by changing chain length of used PVP. When the chain length of PVP was increased, width/length ratio increased, as a result wires was observed. When the long-chain PVP (360K) was used, a longer and a small number of 1-dimensional nanostructures were observed. However, the spherical nanoparticles were formed in the presence of short-chain of PVP (10K). There are several metal nanoparticles such as Iron (Fe), Cobalt (Co), Nickel (Ni), Copper (Cu), Rubidium (Ru), Rhodium (Rh), Palladium (Pd), Silver (Ag), Tin (Sn), Gold (Au) are synthesized with polyol method. 30-200 nm nanoparticles might be obtained by changing experimental parameters with polyol method. Although, the speed of reaction is slower and the reaction time is longer than the reduction of aqueous $NaBH_4$, it provides high yield product. Also, polyol method is simpler and inexpensive than the others methods.
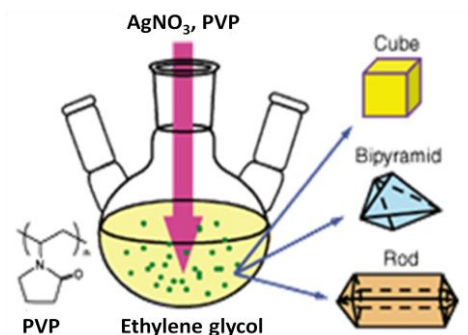
Figure 1.2. Experimental setup of the polyol method
(Source: Tang et al. 2009)

According to mechanism of the polyol method, ethylene glycol is converted to acetaldehyde which reduces Ag^+ to $Ag°$ at high temperatures. However, when PVP is used in this process, firstly Ag^+ ions make complex with PVP, because PVP has strong polar group like C=O bond, so it has affinity to metal ions to form coordinative compounds. After this step, acetaldehyde reduces Ag^+ ions to $Ag°$ and Ag nanoparticles are formed. In Figure 1.3, the schematic diagram of Ag-PVP coordination compound is demonstrated. .
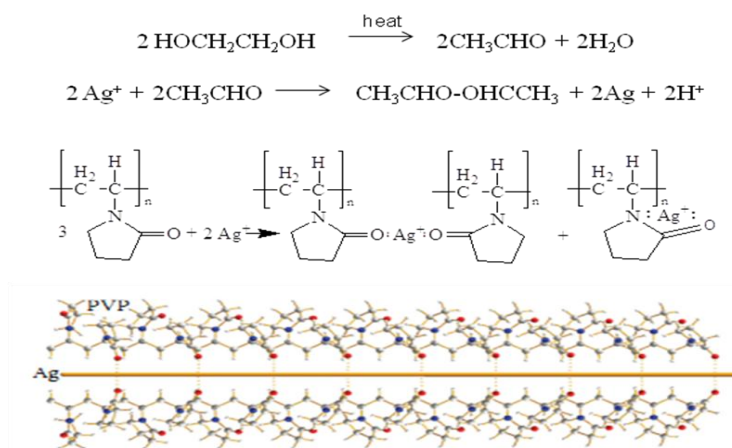
Figure 1.3. The schematic diagram of Ag-PVP coordination compound
(Source: Zhu et al. 2011)

Sun and coworkers synthesized Ag nanowires and nanoprisms by using polyol method. They showed that Ag nanowires and nanoprisms could be produced by reducing $AgNO_3$ with ethylene glycol in the presence of PVP (Sun, Gates, et al. 2002). The properties of the Ag nanowires (dimensions, shape and size) can be controlled by

changing the experimental conditions (temperature, ratio of Ag salt and PVP, etc.). Another example of the polyol method is performed by Roselina and coworkers (Roselina, Azizan, and Lockman 2012). They synthesized nickel nanoparticle by using polyol method.

Microemulsion was first used by T. P. Hoar and J. H. Shulman, professors of chemistry at Cambridge University, in 1943 (Schulman 1943). A microemulsion composes by the presence of normally immiscible two liquid and one or more surfactants in the media. There are different types of microemulsion system such as water-in-oil(w/o), oil-in-water(o/w) and water-in-sc-CO_2(w/sc- CO_2)(Tran et al. 2009). Figure 1.4 shows that different types of microemulsion systems.
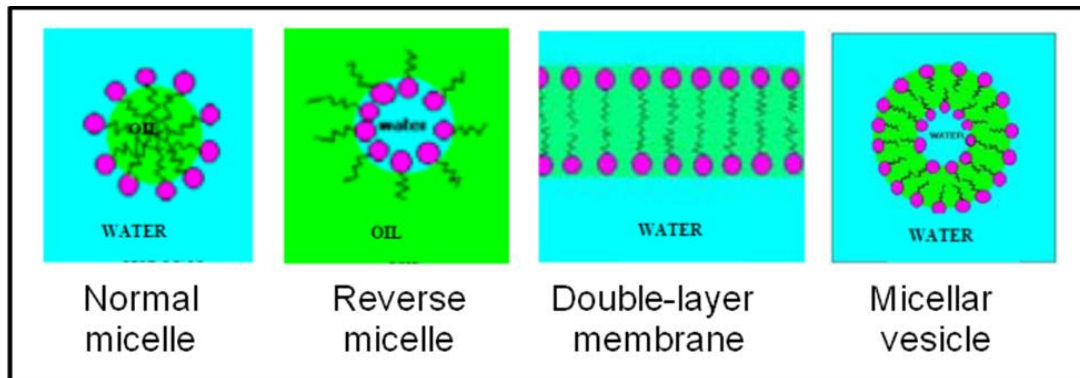
Figure 1.4. Different types of microemulsion system
(Source: Tran et al. 2009)

The ratio of water to concentration of surface active agent (w = $[H_2O]_{mol}$ / $[Surfactant]_{mol}$) is directly control the size of the drops. Also, the size of these drops controls particle size. Microemulsion method is used to obtain materials such as semiconductors, metals and oxides (Zhu, Chen, and Liu 2011, 2012).

Metallic nanoparticles such as Pt, Pd, Cu, Ag, Au, Ni, Zn was prepared with microemulsion method. Advantage of this method is small particle size, high stability and good particle size distribution (Anna Zielińska-Jurek 2012). For instance, Pileni and coworkers synthesized silver nanoparticle by AOT microemulsion (Taleb, Petit, and Pileni 1997). AOT (bis(2-ethylhexyl)sulfosuccinate) which is a anionic surfactants is used to create reverse micelle. It is also said that this reverse micelle is the reaction medium so nanoparticle size depends on the size of this micelles.

Penner's group developed a classical electrochemical method. Electrochemical synthesis is a method to form inorganic deposits on solid surfaces. Although, the mostly used field is the synthesis of semiconductor nanostructure, this method is also used to synthesis of metal nanoparticles which have narrow size distributions. The electrochemical synthesis includes six elementary steps:

✓ Oxidative dissolution of the M_{bulk} anode.

✓ Migration of M^{n+} ions to cathode.

✓ Reductive formation of zero valent metal atoms at the cathode.

✓ Formation of metal nanoparticles.

✓ Regulators, such as tetra-alkyl ammonium salt, prevent the accumulation of particles on the surface of the cathode in the process.

✓ Monodisperse particles with a size of 4 – 8 nm at the end of the reaction is collected and dried.

Figure 1.5 shows that schematic diagram for electrochemical method.

Anode: $\qquad M_{bulk} \longrightarrow M^{n+} + ne^-$

Cathode: $\qquad M^{n+} + ne^- + stabilizer \longrightarrow M_{coll/stabilizer}$

Sum: $\qquad M_{bulk} + stabilizer \longrightarrow M_{coll/stabilizer}$
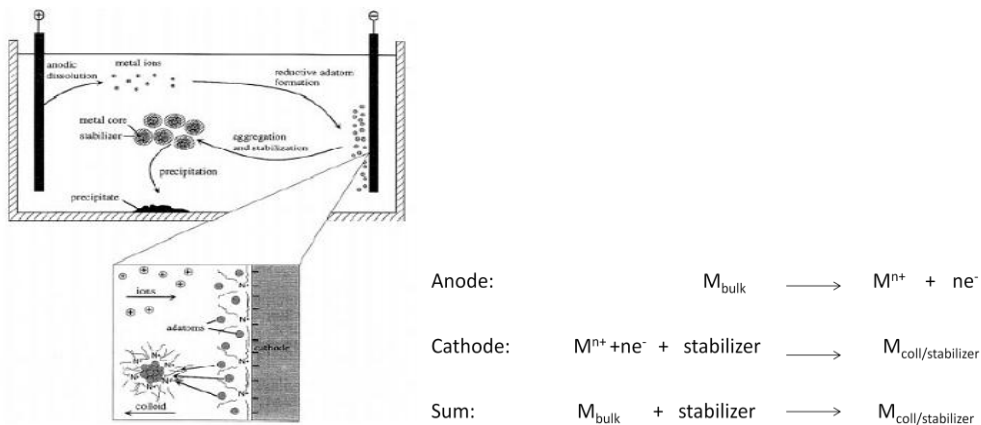
Figure 1.5. Schematic diagram for Electrochemical method
(Source: Bonnemann and Richards 2001)

Different shape of the metal nanoparticle could be synthesized with electrochemical method. To give an example of this method, Yang and coworkers studied with electrochemical method to synthesized copper nanorods (Yang et al. 2003). Besides, Huang and coworkers synthesized gold nanocubes with this method (Huang et al. 2006).

1.3. Spectral Structural Methods of Characterization of Metal Nanoparticles

UV-Vis spectroscopic data provide qualitative and quantitative information of a compound or molecule. In ultraviolet and visible region, in general occurring absorption results from the stimulation of bond electrons. It can be deduced from this phenomena, the wavelengths of absorption peaks can be associated with the investigated types of bonds. According to *Beer's Law* : $\boldsymbol{A = \varepsilon b c}$ $\qquad$ (1.1);

A is absorbance (unitless), ε is the molar absorptivity of the compound or molecule in solution ($M^{-1}cm^{-1}$), b is the path length of the cuvette or sample holder (usually 1 cm), and c is the concentration of the solution (M).

A typical absorption spectrum of Ag nanoparticle is given in Figure 1.6. UV–vis absorption spectrum of silver nanoparticle.
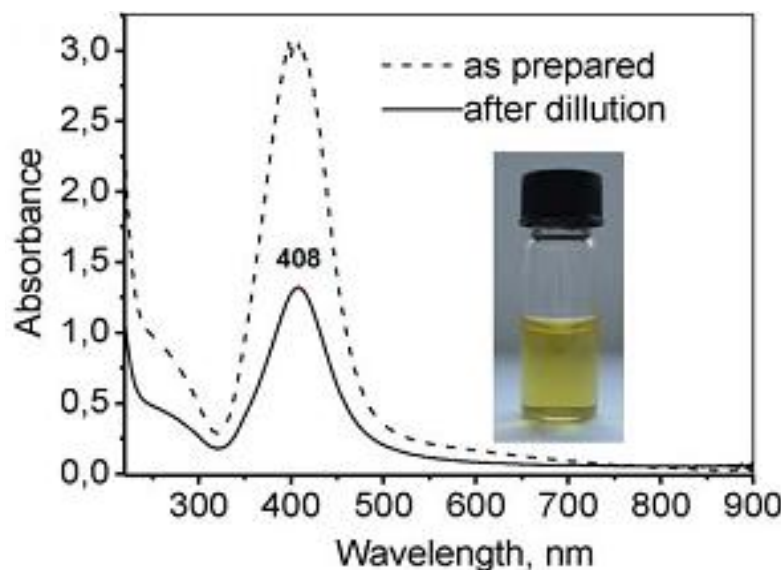
Figure 1.6. UV–vis absorption spectrum of silver nanoparticle
(Source: Vasileva et al. 2011)

In this study, optical characterization of synthesized nanoparticles was determined by using UV-Vis Spectrophotometer. Absorption spectra of silver and silver chloride nanoparticle were recorded by Shimatzu 2550 spectrophotometers.

Structural characterization of synthesized nanoparticles could be determined by using X-Ray Diffraction (XRD), Dynamic Ligth Scattering (DLS) technique, Scanning

Transmission Electron Microscopy (STEM), Scanning Electron Microscopy – Energy Dispersive X-Ray Spectroscopy (SEM-EDS), Transmission Electron Microscopy (TEM).

In this study, the crystalline structure of the nanoparticles were analyzed using an X-ray diffractometer (Philips X'Pert Pro X-Ray Diffractometer) with Cu Kα radiation at IYTE-MAM (Material Research Center). XRD is one of the non destructive technique to inform about the chemical composition, the crystal structure of the nanocrystals, determining the excellence crystalline or purity of the phase, determining the direction of the crystal, determining the crystal lattice constants.

 Basically, principle of operation can be said refraction and diffraction data collection by sending the X-ray to the sample. Scanning Electron Microscopy is essential for understanding information about the sample's surface topography, composition and other properties such as electrical conductivity. Scanning Electron Microscopy was used to determine shape, composition and size of the nanoparticles. Besides, Energy Dispersive X-Ray Detector (EDS) which is used for the elemental analysis or chemical characterization of sample is the most common used accessory of SEM. In this study, Philips XL 30S FEG Scanning Electron Microscope at IYTE-MAM was used for the analysis of nanoparticles. Also Scanning Transmission Electron Microscopy (STEM) at IYTE-MAM and Transmission Electron Microscopy (TEM) at Muğla Sıtkı Koçman University Materials Research Laboratory were used to understand size and shape of the nanoparticles.

Malvern Zetasizer Nanoseries -Nano-ZS Dynamic Light Scattering (DLS) was used to measure the size of the nanocrystals. Generally, DLS measures the size is bigger than TEM or STEM because TEM measures the hard core of the nanocrystal but DLS measures both hard core and hydrodynamic diameter of the nanoparticles (Qian et al. 2007). Solid, liquid and powder even in case of gas can be applied.

1.4.   Purpose of this Study

The aim of this M.Sc. thesis work is to synthesize and characterize a novel composite containing silver chloride (AgCl) nanoparticles and polyaniline (PANI) and to fabricate ECG sensors and evaluating their performances as ECG electrodes.

CHAPTER 2

SYNTHESIS AND CHARACTERIZATION OF SILVER NANOPARTICLES

2.1. Introduction

Metal nanoparticles play important roles in many different areas by means of their tunable physical and chemical properties (Tao, Habas, and Yang 2008). Silver nanostructures have unique electrical, optical and thermal properties depending on particle size, shape and composition (Khan et al. 2011). Their potential usage areas are microelectronic and optoelectronic devices, information storage, medical diagnostics, biological imaging and catalysis (Sun and Xia 2002, Li et al. 2010, Katz and Willner 2004). Also because of the antibacterial property the silver nanostructures are used in many areas. Oxygen metabolism of a virus, bacteria, fungi or other single-cell pathogens are deactivated in the presence of silver, so pathogens die within a few minutes (Ravishankar Rai V 2011).

Several methods, physical and chemical, have been used for the synthesis of silver nanoparticles. The chemical methods are alcohol reduction process (Dekker 2004), microemulsion method (Petit, Lixon, and Pileni 1993), electrochemical synthesis (Mazur 2004), hydrothermal process (Kim 2006) and polyol process (Sun and Xia 2002). These methods were mentioned in Section 1.2. In these methods, the size of silver nanoparticles can be controlled by changing the experimental conditions such as temperature, stirring and injection rate, molarities of silver salt and stabilizer.

There are many studies about synthesis of silver nanoparticles in the literature. One of the most used synthesis method of Ag nanoparticles is the polyol method. Wiley and coworkers (Wiley et al. 2004a) were used this method to synthesize different sized (particle size is in the range of 20 to 80 nm) and various shaped (such as cubic and tetrahedrons) single silver nanocrystals by changing the experimental parameters. Another study of Xia et al. demonstrated that cube, rod/wire and sphere silver nanoparticles could be synthesized by means of using different capping agents, controlling concentration of the silver salt ($AgNO_3$) and varying the molar ratio of silver

precursor and the capping agent in the polyol process (Wiley et al. 2005). Li et al. synthesized monodispersed Ag NPs (25, 35, 45, 60 and 70 nm) by changing the reaction temperature, the reaction time, the concentration of the surfactant and the reactants in the polyol method in 2012. They used these Ag NPs to evaluate cytotoxicity against human lung fibroblast cells. As a result of this study, they found that the cytotoxicity increased significantly upon decreasing the size of the Ag NPs and increasing the doses of Ag NPs (Li et al. 2012). Sun and coworkers synthesized uniform, bicrystalline silver nanowires (diameters in the range of 30-40 nm, and lengths up to 50 μm) by using the polyol method. They synthesized Pt nanoparticles by reducing $PtCl_2$ with ethylene glycol at high temperature (at 160°C). As seeds for Ag nanoparticles they used these Pt nanoparticles as a seed for the growth of Ag nanoparticles because crystal structure and lattice parameters for Pt and Ag are very close. As a result, they obtained 20-30 nm Ag nanoparticles. They kinetically controlled the growth rates by using PVP (Sun, Yin, et al. 2002). Wiley and coworkers obtained silver nanobars and nanorices by adding different concentrations of NaBr to the reaction medium (Wiley et al. 2007).

Solomon and coworkers studied the synthesis of silver nanoparticles by using $NaBH_4$, which is a reducing agent without stabilizer (S. D. Solomon and Boritz 2007). The stability of Ag nanoparticles was investigated depending on the molar ratio of $NaBH_4$ and $AgNO_3$. They observed that when the molar ratio is two, these Ag nanoparticles are more stable and the size of these particles is 12 nm. Yi et al. prepared Ag nanoplates (40 nm to 260 nm) in order to assess the SERS enhancement. They used two reducing agents ($NaBH_4$ and sodium citrate) to obtain silver nanoplates (Yi et al. 2013).

Silver nanoparticles were synthesized by various physical methods as well. For instance, Xu and coworkers synthesized highly fluorescent, stable and water soluble Ag nanoclusters with sonochemical synthesis (Xu and Suslick 2010). Petit and coworkers prepared monodisperse and stable Ag nanoparticles by using reverse micelles. They controlled the size of these particles with the number of initiators per micelle in this study (Petit, Lixon, and Pileni 1993). In another study, Kang et al. synthesized dodecanethiol-derivatized Ag nanoparticle with one-phase and two-phase methods at -18 ℃ (Kang and Kim 1998).

The studies exemplified above points out that size and shape of Ag nanoparticles can be tuned by controlling reaction conditions such as temperature, concentration of reactants and surfactants.

In this thesis work, the silver nanoparticles were synthesized by two different methods. First one is the polyol method and the second one is the reduction of silver salt in the presence of $NaBH_4$. Various sized (from 2.5 to 150 nm) and different shape silver nanoparticles were synthesized by using these two methods.

2.2. Experimental

In this study, Ag nanoparticles were synthesized by means of two methods. The first method is the reduction of silver salt with $NaBH_4$ and the second method is the polyol method. These two methods were used because these are relatively easy, not expensive and less toxic compared to other methods that were used in the literature.

2.2.1. Reagents

All chemicals used were of the highest purity available. As a metal source silver nitrate ($AgNO_3$, Sigma-Aldrich 99%) was used throughout the study. Ethylene glycol ($HOCH_2CH_2OH$, 99.8%) was purchased from Sigma-Aldrich. Sodium borohydride ($NaBH_4$, 99%) was purchased from Merck. Poly(vinylpyrolidone) (PVP) (M.W.$\approx$ 8,000) was purchased from Alfa-Easer. Deionized (DI) water was used throughout the study.

2.2.2. Synthesis of Silver Nanoparticles

2.2.2.1. The Reduction of Silver Salts with $NaBH_4$

Silver nanoparticles were synthesized by the chemical reduction of silver nitrate. $NaBH_4$ is a strong reducing agent. In the presence of $NaBH_4$, $AgNO_3$ salts were easily reduced, and small-sized Ag nanoparticles (sizes < 10 nm) were synthesized.

$$AgNO_3 + NaBH_4 \longrightarrow Ag + \frac{1}{2} H_2O + \frac{1}{2} B_2H_6 + NaNO_3 \qquad (2.1)$$

First, 30.0 ml of 2.0 mM sodium borohydride ($NaBH_4$) solution was chilled at -18 ℃ during 30 minutes. Chilled $NaBH_4$ solution is very important to limit the rate of hydrolysis. 10.0 ml of 1.0 mM $AgNO_3$ and 2.0 ml of 0.5 mM PVP were dissolved in

ultra-pure water in two different beakers separately at room temperature. After sodium borohydride (NaBH$_4$) solution was chilled, 10.0 ml AgNO$_3$ was added to 30 ml NaBH$_4$ solution in an ice-bath and then 2.0 ml PVP solution was injected to this solution. The mixture was stirred vigorously to form Ag nanoparticles. After 5 minutes, the color of solution turned into brighter yellow. The change of color was the indication of formation of Ag nanoparticles. These colloidal silver nanoparticles are highly stable and had been stored for more than one year in the dark and at 4 ºC. Figure 2.1 illustrates the synthesis of Ag nanoparticles by the reduction of AgNO$_3$ by NaBH$_4$.
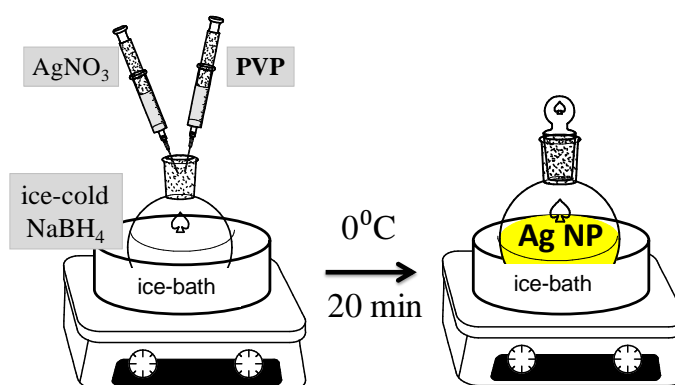
Figure 2.1. Schematic illustration of synthesis of the Ag nanoparticles by the reduction of AgNO$_3$ by NaBH$_4$.

2.2.2.2. The Polyol Method

The Polyol method is the second method we used to synthesize Ag nanoparticles. One of the reasons for the popularity of the polyol method is that it allows to work at high temperatures because the boiling point of ethylene glycol is 197 ºC. The method works for a wide range of temperature. In this method, first, 5.0 ml ethylene glycol was heated in a two-necked flask for one hour, at 80 ºC. 0.125 M AgNO$_3$ and 0.75 M PVP were dissolved in ultra-pure water separately at room temperature. These separately prepared solutions were simultaneously added into the ethylene glycol at 80 ºC drop by drop. Then, the solution was stirred at 500 rpm for 25 minutes. After 25 minutes, spherical Ag nanoparticles were formed. Two different temperatures which were 160 ºC and 170 ºC were applied to for the same reactant concentrations to increase the reducing power of ethylene glycol. The shape of particles

was transformed to wire by increasing the reaction temperature. After the reaction was completed, the solution was cooled down to the room temperature to stop the growth of Ag nanoparticles. Figure 2.2 illustrates the synthesis steps of Ag nanoparticles via the polyol method schematically.
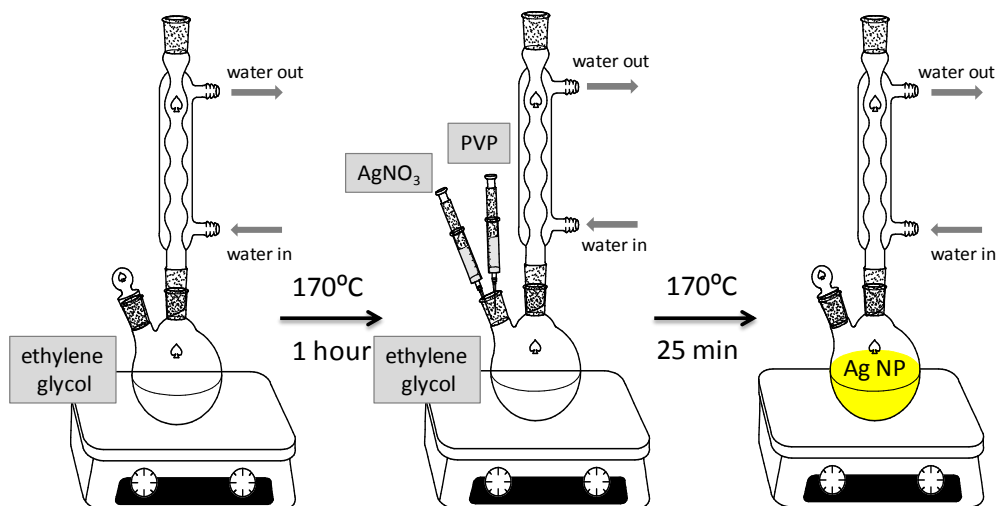
Figure 2.2. Schematic illustration of the synthesis of Ag nanoparticles by polyol method.

2.3. Results

Spectral characterization of the Ag nanoparticles was performed by Ultraviolet-visible absorption spectroscopy. UV-vis spectra are used to monitor how the reaction proceeds. Dynamic light scattering (DLS) measurements and scanning electron microscopy respectively were used to measure size and size-distribution and to assess the shape of the Ag nanoparticles.

2.3.1. Spectral and Structural Characteristics Ag Nanoparticles Prepared by the Reduction of AgNO$_3$ with NaBH$_4$

In this section, the effect of the amounts of capping agent and the reducing agent on the particle size was investigated.

In Figure 2.3, the effect of PVP amount on the size of Ag nanoparticle was shown. When no PVP was used, the typical absorption due to localized surface plasmon

band of Ag nanoparticle at 400 nm was slightly observed with one broad band at 535 nm was appeared. When PVP was used as a capping agent, a typical absorption band of Ag nanoparticle was observed at 400 nm. However, as the amount of PVP was increased in the medium, the absorbance decreased and the band broadening was observed. The size of non-agglomerated Ag nanoparticle was measured with dynamic light scattering. It was observed that the size of the Ag nanoparticle was increased from 1.8 nm to 5.8 nm, when the volume of PVP was increased from 1.0 to 6.0 ml (Figure 2.4).
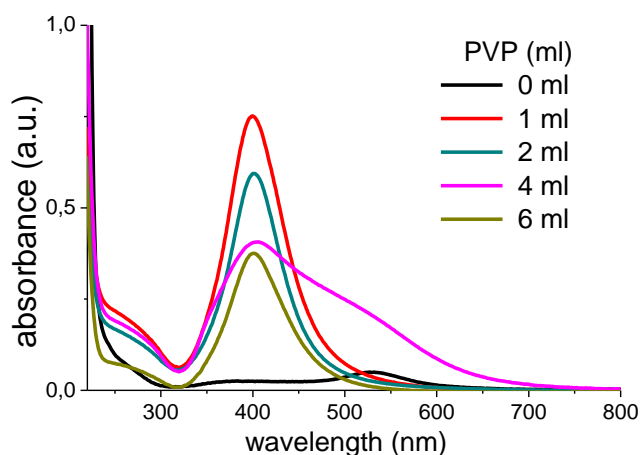
Figure 2.3. Absorption spectrum of Ag nanoparticles with different volume 0 ml, 1 ml, 2 ml, 4 ml, 6 ml of 0.5 mM PVP.
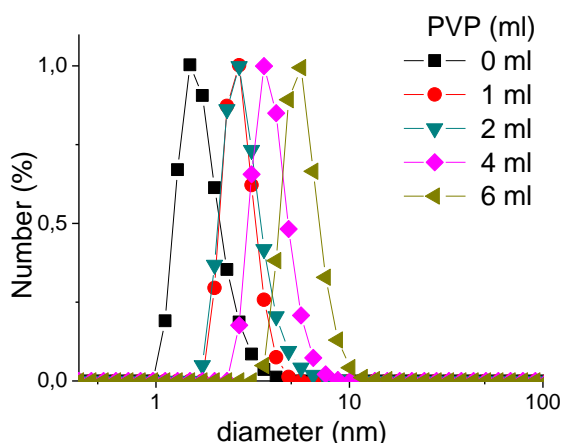
Figure 2.4. Size distribution of the Ag nanoparticle with different volume 0 ml, 1 ml, 2 ml, 4 ml, 6 ml of 0.5 mM PVP.
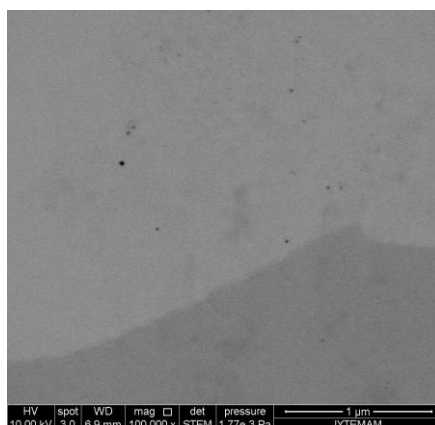
Figure 2.5. STEM image of Ag nanoparticles.

Figure 2.5 shows the STEM image of Ag nanoparticle. It is apparent that size of Ag nanoparticle measured by STEM is larger than that of Ag nanoparticle determined by DLS result (2.9 nm). Here, cluster of Ag nanoparticles were observed. Actually, the size measured by DLS should be bigger than the STEM measurement because DLS measures the hydrodynamic diameter of nanoparticles, while microscopy determines the crystalline size.
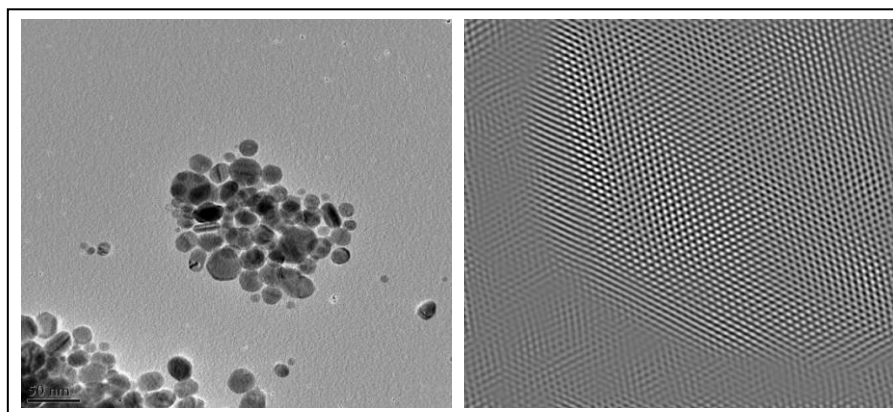
Figure 2.6. HRTEM image of Ag nanoparticles.

Figure 2.6 shows both TEM and HRTEM images of the Ag nanoparticles. HRTEM image of the Ag nanoparticles shows that the nanoparticles have well-ordered face-centered cubic (fcc) structure and lattice constant of the crystals is 4.090 Å.

To evaluate the effect of the amount of the reducing agent, the volume of 2.0 mM $NaBH_4$ was varied from 20 ml to 50 ml. The effect is reflected on the absorption

spectra as narrowing of the band as seen in Figure 2.7. In addition, the size of the particles increased from 2.3 nm to 3.6 nm (Figure 2.8).
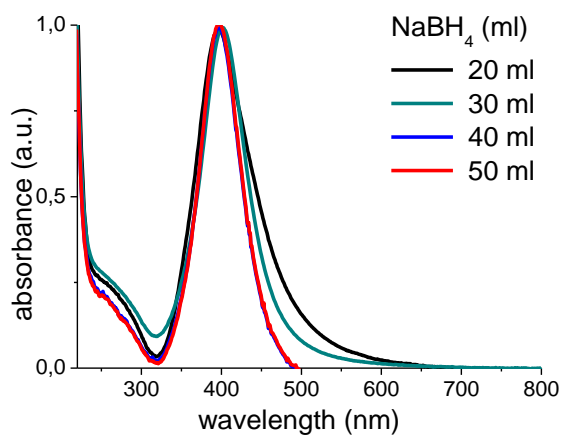
Figure 2.7. Absorption spectrum of Ag nanoparticles with different volume 20 ml, 30 ml, 40 ml, 50 ml of 2.0 mM NaBH₄.
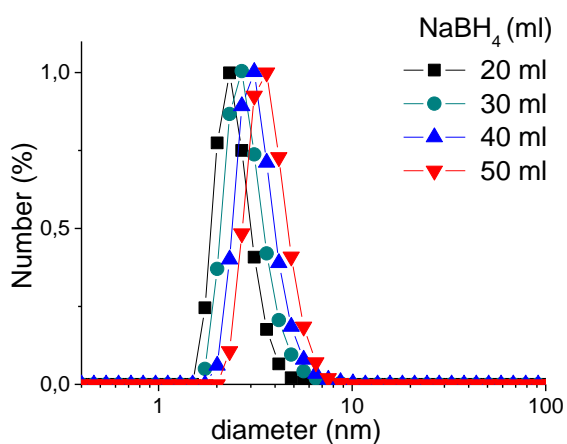
Figure 2.8. Size distribution of the Ag nanoparticle with different volume 20 ml, 30 ml, 40 ml, 50 ml of 2.0 mM NaBH₄.

In another set of the experiment, the Ag nanoparticles was synthesized by doubling the total volume to examine whether the scale-up experiment is possible or not.
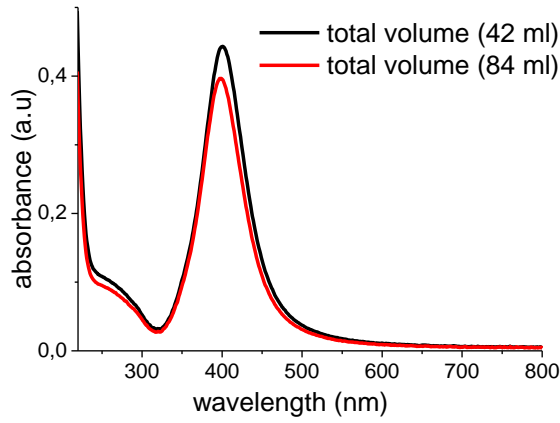
Figure 2.9. Absorption spectrum of Ag nanoparticles, the total reaction volume was doubled.

Figure 2.9 demonstrates that, when the total reaction volume was doubled, the absorbance peak at 400 nm slightly decreased. The size measurements by DLS (Figure 2.10) showed that the size of the Ag nanoparticles was not different. No profound change on the shape of optical spectra of the nanoparticles was observed. To determine the concentration of nanoparticles in different reaction volume, we used the formulation given below (Liu et al. 2007).

$$N = \frac{\pi}{6} \rho \frac{D^3}{M} N_A \quad \text{and} \quad C = \frac{N_{Total}}{N \, V N_A} \tag{2.2}$$

Where N is the number of atoms per nanoparticle, ρ is the density of silver, D is the average diameter of nanoparticles, M is the atomic mass of silver, N_A is Avogadro's number, V is the volume of the reaction solution. By taking the D is 2.5 nm and 2.9 nm (DLS measurement), ρ is 1.05×10^{-20} g/nm^3, M is 108 g/mol, N_A is 6.022×10^{23} atoms/mol and V are respectively 42 and 84 ml, we calculated the number of silver atoms per particle (N) and the number of silver particles per cm^3 as follows:

Table 2.1. Calculation of the number of particles per cm^3 depending on reaction volume

Size (nm)	N (the number of silver atoms per particle)	C (the number of silver particles per cm^3)
2.9±0.7 nm Volume = 42 ml	750 atoms/NP	2.0×10^{17} NP/cm^3
2.5±0.5 nm Volume = 84ml	500 atoms/NP	3.0×10^{17} NP/cm^3

It can be considered that the scaling-up is possible for the synthesis of Ag nanoparticles without changing the optical properties by increasing the reaction volume. When the reaction volume was doubled, the concentration of the particles per cm^3 increased about one and half times, but not doubled.
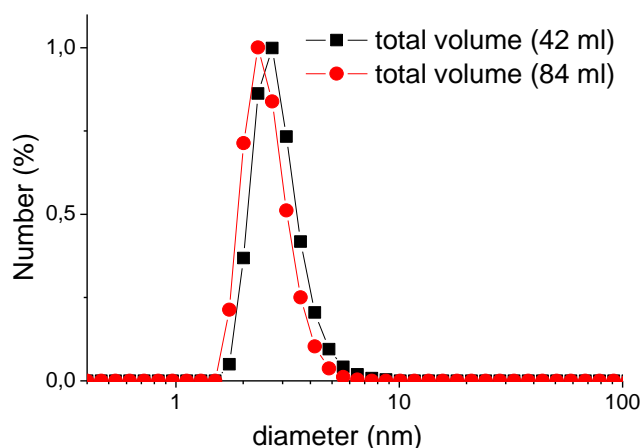
Figure 2.10. Size distribution of the Ag nanoparticles by doubling the total reaction volume.

2.3.2. Spectral and Structural Characteristics Ag Nanoparticles Prepared by the Polyol Method

In this part, the effects of amount of AgNO$_3$, amount of PVP and temperature on the size and shape of the Ag nanoparticles were examined.

First, the concentration of AgNO$_3$ (0.125 M) and the reaction temperature (80 ºC) were kept constant, but the concentration of PVP was changed. Table 2.1 shows the variation in the amount of PVP.

Table 2.2. Change in the PVP amounts

AgNO$_3$ (M)	EG (ml)	Temp (ºC)	PVP (M)
0.125	5	80	0.375
0.125	5	80	0.500
0.125	5	80	0.750

Wide bands in the UV-Vis spectra were observed in Figure 2.11 and Figure 2.12 shows that the distribution is enlarged as well. The reason for the larger width is assigned to polydispersity of the nanoparticles. Actually, it is difficult to obtain a monodisperse distribution of metal nanoparticles because these particles form (nucleate) very fast. However, when the molarity of PVP was increased, UV-vis absorption spectra and dynamic light scattering distribution was narrowed slightly (Figure 2.11 and Figure 2.12). In Figure 2.13, SEM images confirm the polydispersed nature of the nanoparticles. The images prove that the shapes of the particles are spherical. Figure 2.12 shows that the particle size under each PVP molarity is nearly same, approximately 170±70 nm.
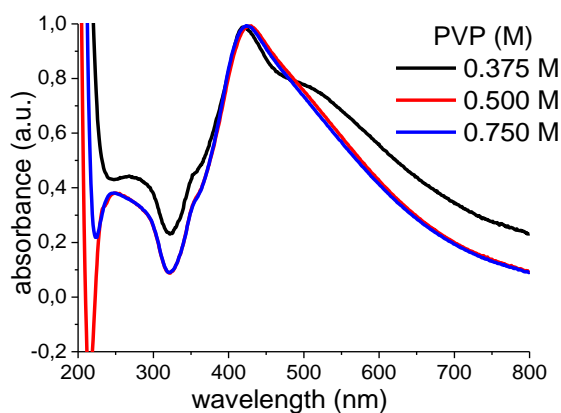
Figure 2.11. Absorption spectrum of Ag nanoparticles with different molarity of PVP.
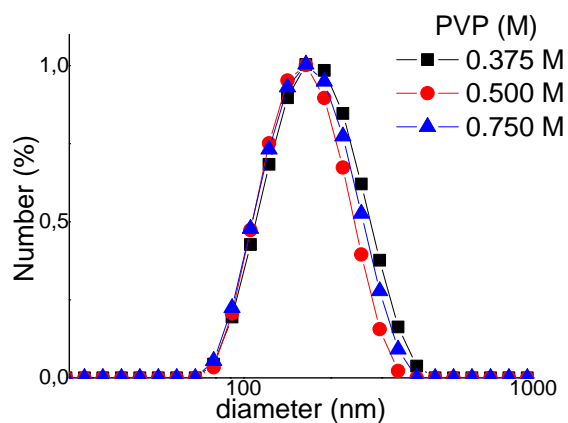
Figure 2.12. Size distribution of the Ag nanoparticle with different molarity of PVP.
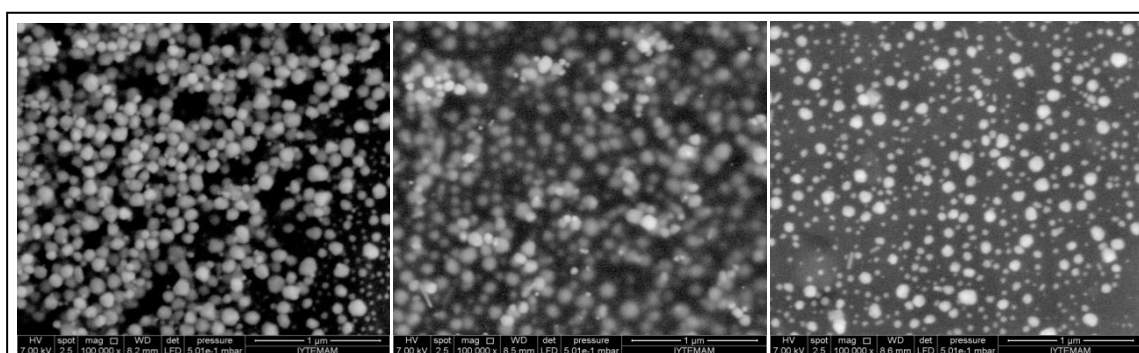
Figure 2.13. SEM images of a) 0.375 M PVP and b) 0.50 M PVP c) 0.75 M PVP.

After optimizing PVP concentration at 80 °C, the effect of amount of $AgNO_3$ was investigated. The amount of silver nitrate was doubled. Figure 2.14 shows the absorption spectra of Ag nanoparticles was obtained by using 0.125 M and 0.250 M silver nitrate and 0.750 M PVP at 80 °C. Here, when the concentration of the silver nitrate increases from 0.125 M to 0.250 M at 80 °C, the narrower band was observed and the peak position was shifted to blue region.
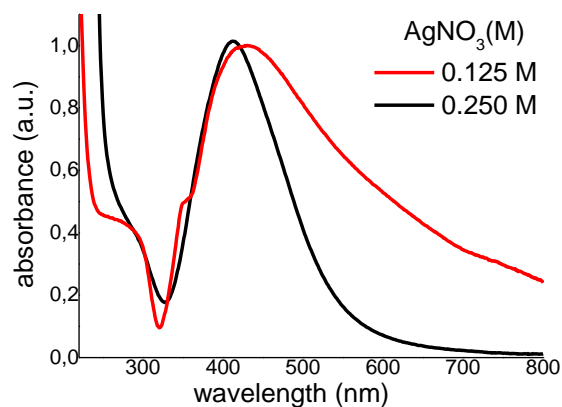
Figure 2.14. Absorption spectrum of Ag nanoparticles with different concentration of silver nitrate.
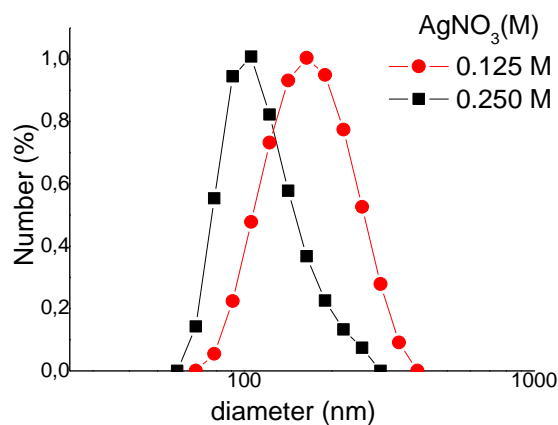
Figure 2.15. Size distribution of the Ag nanoparticle depending on different molarity of silver nitrate.

Figure 2.15, the dynamic light scattering measurements indicate the broader nature of the particles size synthesized under both silver nitrate concentration (0.125 M and 0.250 M). When 0.125 M silver nitrate was used, the particles are spherical but the size of the particles is not same (Figure 2.16.a). However, according to Figure 2.15 the particle size decreased as a result of increase in $AgNO_3$ concentration from 0.125 M to 0.250 M. SEM images of the particles show that monodispersed spherical nanoparticles were formed under high concentration of silver salt, 0.250 M $AgNO_3$ (Figure 2.16.b).
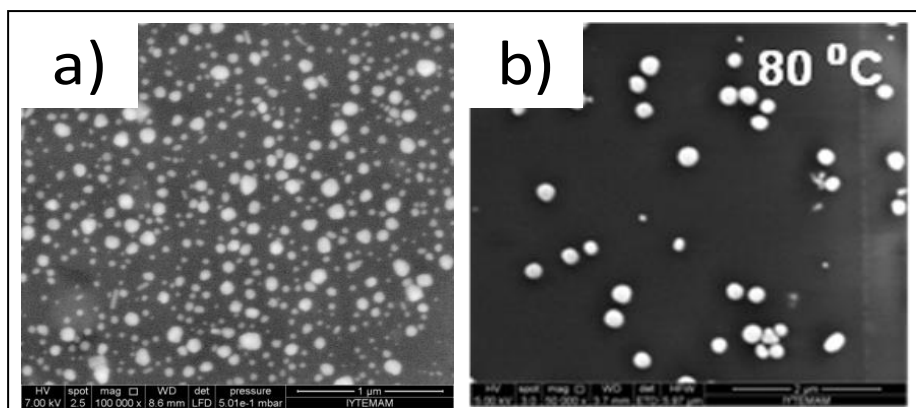
Figure 2.16. SEM images of Ag nanoparticles synthesized with a) 0.125 M AgNO$_3$ and
b) 0.25 M AgNO$_3$.

The reaction temperature is an important parameter in the polyol method for Ag nanoparticle synthesis. The reaction temperature can greatly influence reaction rate, therefore size and shape of the particles can be affected by the temperature. Table 2.2 show the reaction temperature was varied.

Table 2.3. Change in the reaction temperature

AgNO$_3$ (M)	PVP (M)	EG (ml)	Temp (ºC)
0.25	0.75	5	80
0.25	0.75	5	160
0.25	0.75	5	170

Absorption spectra of the Ag nanoparticles prepared at different temperatures were shown in Figure 2.17. Figure 2.17 shows that Ag nanoparticle absorbed light at 412 nm when the reaction temperature was 80 ºC. However, when the reaction temperature was increased to 160 ºC, the band position was shifted to 427 nm. When Ag nanowires synthesized at 170 ºC, the absorption band appeared at 438 nm. Significant red shift and broadening were observed in Figure 2.17 due to the changes in the morphology of the silver nanoparticles: spherical to wire. The variation in particle shape with temperature was shown in Figure 2.19. Three different particle morphologies were observed at 80, 160 and 170 ºC without changing the molarity of AgNO$_3$ and PVP. The molarity of AgNO$_3$ is 0.25 M and molarity of PVP is 0.75 M.
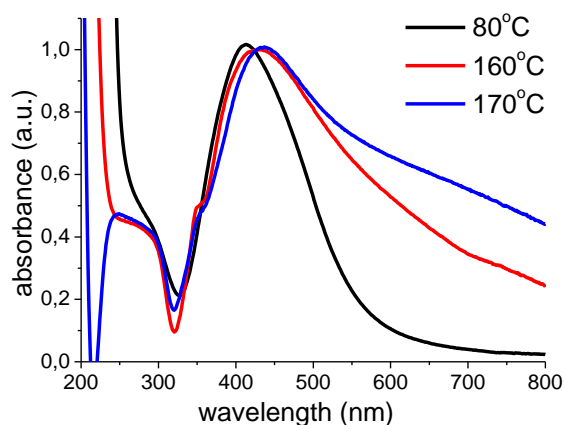
Figure 2.17. Absorption spectrum of Ag nanoparticles at different temperatures.

At 80 ℃ the size distribution of the nanoparticles was narrow. However, as the temperature changes from 80 to 170 ℃, the size and size distributions were varied (Figure 2.18).
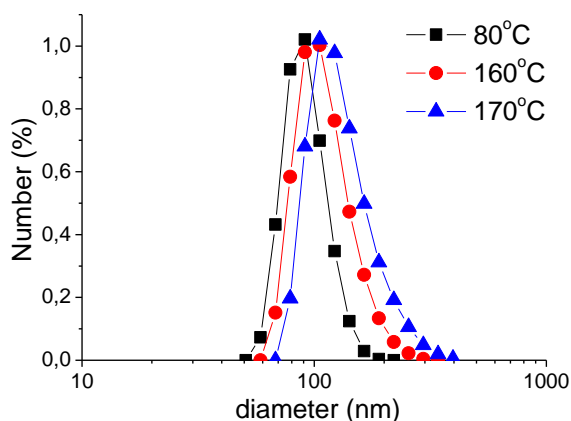
Figure 2.18. Size distribution of the Ag nanoparticle at different temperatures.

SEM images of the nanoparticles support the observations of UV-Vis absorption spectra and DLS results. In Figure 2.19.a, it is seen that the particle shape is spherical. The size of synthesized particles at 80 ℃ is close to each other and the size distribution is highly monodispersed. Figure 2.19.b shows that as the reaction temperature increases to 160 ℃, nanocubes and nanowires were formed. When the temperature was increased to 170 ℃, the shape of particles completely turned to wires, which were shown in Figure 2.19.c.
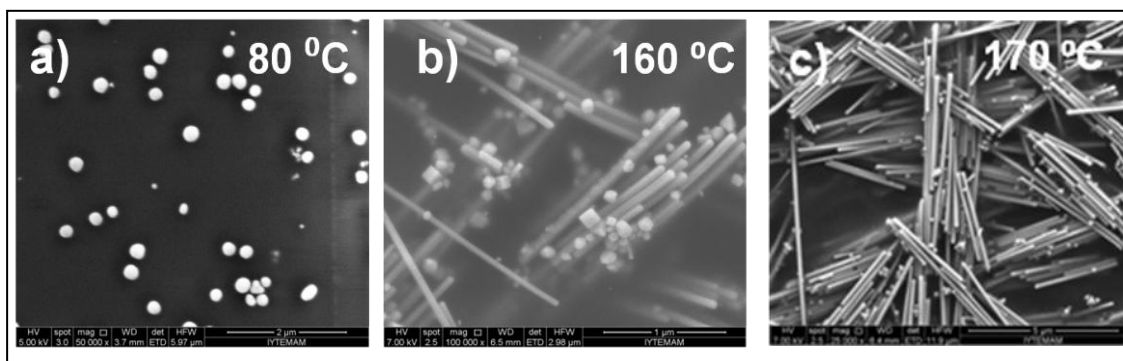
Figure 2.19. SEM images of Ag nanoparticles at a) 80 °C and b) 160 °C c) 170 °C.

2.4. Discussion

We demonstrated the effect of reaction conditions on the particle morphology and the size of particles in this study. In literature, there are many studies about synthesis of silver nanoparticles by different methods. However, we prefered only two methods, the reduction of $AgNO_3$ by $NaBH_4$ and the polyol method. For the synthesis of Ag nanoparticles we compared the methods regarding to the size and the shape of the particles.

Dong et al. reported that small spherical silver nanoparticles were prepared by the rapid reduction of the precursor with $NaBH_4$ at ice-bath temperature (Dong et al. 2010). As Dong's study, we obtained smaller than 10 nm spherical Ag nanoparticles by using $NaBH_4$ as the reducing agent. We studied the effects of amount of the reducing agents on the particle size. We showed that increasing the $NaBH_4$ caused an increase in the size of the particles. Although we slightly increased the concentration of $NaBH_4$ in total solution volume (1.25 mM to 1.61 mM), the size of the particles significantly increased from 2.3±0.5 nm to 3.6±0.9 nm. Rafique and coworkers showed similar effect of the $NaBH_4$ concentration on size of $CoFe_2O_4$ nanoparticles (Rafique et al. 2012).

To evaluate the protecting ability of PVP and its concentration, on the agglomeration we synthesized Ag nanoparticles at different concentrations of PVP. However, contrary to the literature, we observed the size of the particles increased, when the concentration of PVP was increased upto 0.06 mM. Whereas PVP prevents agglomeration due to the steric effect (Wang et al. 2005), according to DLS and Uv-Vis spectra results, when 1.0 or 2.0 ml of 0.05 mM PVP was added to reaction, the size of silver nanoparticles was not changed, but narrower absorption bands were observed.

However, when we increased the concentration of PVP in the medium, the size of silver particles increased. Therefore we determined that the optimum amount of PVP is 2 ml of 0.05 mM PVP solution that prevents agglomeration in our study. We observed that the clusters started to form in the medium, when the amount of stabilizer increased more (Malina et al. 2012).

Actually, it is not easy to control the shape and the size of Ag nanoparticles in aqueous phase because the nucleation and growth are very fast (Wan et al. 2013).

Table 2.4. Synthesis conditions for the preparation of silver particles using the polyol method.

Shape	Polyol	$AgNO_3$ (M)	PVP (M)	PVP/$AgNO_3$	T/°C	Size (nm)	
spherical	EG	0.125	0.375	3:1	80	175±80	(polydisperse)
	EG	0.125	0.500	4:1	80	161±69	
	EG	0.125	0.750	6:1	80	165±78	
spherical	EG	0.250	0.750	3:1	80	95±23	(monodisperse)
cube/wire	EG	0.250	0.750	3:1	160	100±31	
Wire	EG	0.250	0.750	3:1	170	175±80	

We observed that controlling the shape and the size of silver nanoparticles using the polyol method is doable. When the PVP concentration was increased, the size of Ag nanoparticles decreased. Because of increasing the amount of PVP in the reaction medium, the rate of spontaneous nucleation increases and a higher number of nuclei are formed (Carotenuto, Pepe, and Nicolais 2000). Hence, the total number of particles increases and the mean particle size decreases. It can be proposed that PVP plays an important role in the control of size of Ag nanoparticles. Papp and coworkers showed that in the presence of polymer stabilizer, the average particle size decreases and the distribution is less polydispersed because the particles are sterically stabilized by PVP and the nucleation rate is hindered and the growth rate is slowed in the presence of PVP (Papp, Patakfalvi, and Dekany 2007). Contrary to Papp's study, although we increased the amount of PVP, the shape of our Ag nanoparticles was not altered but polydispersed size distributions were observed.

We studied effect of amount of $AgNO_3$ as well by doubling the amount of $AgNO_3$ because Nguyen and coworkers reported that size and size distribution of the silver nanoparticles strongly depended on silver cations in the initial reaction solution (Nguyen V. Nghia 2002) . When the concentration of silver nitrate was increased, the

size distribution of the particles was monodispersed and the size of the particles was less than 100 nm. After, we examined the effect of stabilizer and metal source concentrations, we studied that the effect of temperature. We observed spherical particles but no nanowires at 80 °C, because at 80 °C thermal energy is not enough for the formation of particles which tends to grow along the {111} planes to form rod-shape and wire-shaped particles (Coskun, Aksoy, and Unalan 2011, Sun, Yin, et al. 2002). However, when the temperature was increased to 160 °C, the shape of Ag nanoparticles changed from spherical to wire/cube. However, at 160 °C, the shape of silver nanoparticles was not transformed completely to wire due to not enough thermal energy. Therefore, we increased the reaction temperature to 170 °C for the available thermal energy in order to form Ag nanowires.

2.5. Conclusion

We reexamined the methods to synthesize different sized and shaped silver nanoparticles by using the reduction by $NaBH_4$ and the polyol method. We compared the two methods of the synthesis of silver nanoparticles in our reaction conditions. If $NaBH_4$ is used as a reducing agent, the size of the particles is less than 10 nm and the shape of Ag nanoparticles is spherical. However, in the polyol method we obtain different shaped nanoparticles depending on the temperature, and the size of silver nanoparticles is bigger than the 50 nm.

In these two methods, the size of Ag nanoparticles can be tuned depending on the PVP concentration. In the polyol method, polydispersed size distributions were observed by increasing $AgNO_3$ concentration. We obtained different morphologies of the particles like spherical, cube and wire depending on the temperature. The spherical Ag nanoparticles can be synthesized at 80 °C, but the size distribution was polydispersed at this temperature. When the reaction temperature is increased to 170 °C, only Ag nanowires are obtained, because the thermal energy is sufficient to prepare Ag nanowire. The synthesized Ag nanoparticles will be used for biomedical purposes. They will be treated with HCl to obtain silver chloride (AgCl) nanoparticles. After synthesized AgCl nanoparticles, they will be used to coat ECG electrode surface.

CHAPTER 3

SYNTHESIS AND CHARACTERIZATION OF AgCl NANOPARTICLES

3.1.   Introduction

Silver halides (AgX, X=Cl,Br) which have unique optical properties attract attention because of their utilization as optical and photographic material (Belloni 2003). Silver chloride, AgCl, is a stable photosensitive semiconductor material, having a direct bandgap of 5.15 eV (241 nm) and an indirect bandgap of 3.25 eV (382 nm) (Glaus and Calzaferri 2003). That's why AgCl can be used for fabrication of photochromic lenses and photographic paper (Kim et al. 2010, An, Peng, and Sun 2010). Also, it is well known that silver chloride can be used in reference electrode because it is simple, inexpensive, very stable and non-toxic. There are several methods for the synthesis of silver chloride nanoparticles such as light irradiation (Choi, Shin, and Jang 2010) and solvothermal process (Han et al. 2011). Also, silver chloride nanoparticles are synthesized by reduction of $AgNO_3$.

Choi et al. prepared silver chloride/silver nanostructures by using light irradiation. They reported formation of Ag layer on the AgCl nanoparticle providing a separated electron-hole region. In this way, they obtained excellent photocatalytic activity (Choi, Shin, and Jang 2010). Another example for use of the silver chloride nanostructures is illustrated by the study of Kim and coworkers. Kim et al. synthesized morphology controlled silver chloride nanocubes. They reported that the morphology could be important for materials, in applications of biomedical devices, SERS and photocatalysis. Also, they studied the effect of reducing agents on the morphology of the AgCl nanocubes (Kim et al. 2010).

In an another study, Sun and coworkers successfully fabricated AgCl nanowire by using template method (Sun, Chen, and Zhou 2007). They used gelatin as a protector and stuffing to obtain smooth AgCl nanowires which have high aspect ratio. Abbasi et al prepared AgCl nanoparticles by dipping steps under ultrasound irradiation (Abbasi, Bohloulzadeh, and Morsali 2011). They reported that the textile samples containing

AgCl nanoparticles show antibacterial activity for Escherichia coli. Peng and coworkers studied ripening of AgCl nanoparticles at high temperature (160°C) by using polyol method (Peng and Sun 2011). They demonstrated that AgCl nanoparticles exhibit monodispersed size distribution and cube-tetrapod morphology. In addition to this, they reported at high temperature AgCl nanoparticles reduces partially to form Ag on the surface of AgCl nanoparticles due to enhancing reducing properties of ethylene glycol.

One of the purpose of this thesis is to synthesize and characterize silver chloride nanostructures, which may be suitable for biomedical applications such as ECG electrodes.

3.2. Experimental

AgCl nanoparticles were synthesized by using two different methods. The first method is based on the direct addition of HCl. Ag nanoparticles, which were synthesized by the reduction of metal salt method in section 2.2.2.1. The second method to synthesize of AgCl nanoparticles by utilizing the polyol method followed by the HCl treatment.

3.2.1. Reagents

Metal source, silver nitrate (99%) (AgNO$_3$) was purchased from Sigma-Aldrich. Anhydrous ethylene glycol (99.8%), HCl (37%) and poly (vinylpyrolidone) (PVP) (M.W.$\approx$ 8,000) were purchased from Sigma-Aldrich and Alfa-Easer, respectively. Deionized (DI) water was used throughout the study.

3.2.2. Synthesis of Ag Nanoparticles

Silver nanoparticles were synthesized by using the polyol method. The first reaction is the reduction of AgNO$_3$ by ethylene glycol having different concentrations in the presence of the PVP at the room temperature. In a typical synthesis, AgNO$_3$ and PVP were dissolved in 50 ml ethylene glycol in a 100 ml round-bottom flask at the room temperature. The mixture was allowed to stir for 5 min after dissolving process. Figure 3.1 shows the picture Carousel Multiple Synthesis System in which the synthesis

of Ag nanoparticles was carried out. The color of the dispersion of Ag nanoparticles was yellow, indicating the formation of the nanoparticles.

Figure 3.1. Photograph of carousel multiple synthesis system

3.2.3. Synthesis of AgCl Nanoparticles

AgCl nanoparticles were synthesized by the treatment of Ag nanoparticles with HCl at 100 °C. The Ag nanoparticles with the size of 2.9 nm were synthesized by reduction of silver salt as explained in the chapter 2. After Ag nanoparticles were synthesized by this method, HCl was injected to this dispersion at room temperature. Then, this dispersion was heated to 100 °C. In another method, after Ag nanoparticles were synthesized by the polyol method, HCl was added to this dispersion. Then, the dispersion was heated to 100 °C and stirred for 20 min so as to obtain AgCl nanoparticles. After the reaction, the color of the dispersion was turned into white, showing that the synthesis of AgCl nanoparticles. The white dispersion as shown in Figure 3.2 was left to cool to the room temperature by itself. The AgCl nanoparticles were washed three times with 50% acetone and 50% distilled water mixture to remove excess PVP and ionic species. The purified nanoparticles were then dried under vacuum at the room temperature for 48 h for further characterization.

Figure 3.2. Synthesis of AgCl nanoparticles by using carousel multiple synthesis system, The color of the dispersion of AgCl nanoparticles was white.

3.3.   Results and Discussion

3.3.1. Optical and Structural Characterization

In this section, the synthesized AgCl nanostructures were optically and structurally characterized. Optical characterization of the synthesized AgCl nanoparticles by reduction of silver nitrate indicates that Ag nanoparticles were not completely turned to AgCl nanoparticles. Figure 3.3 shows the characteristic Uv-Vis absorption peaks of the Ag and AgCl nanoparticles.
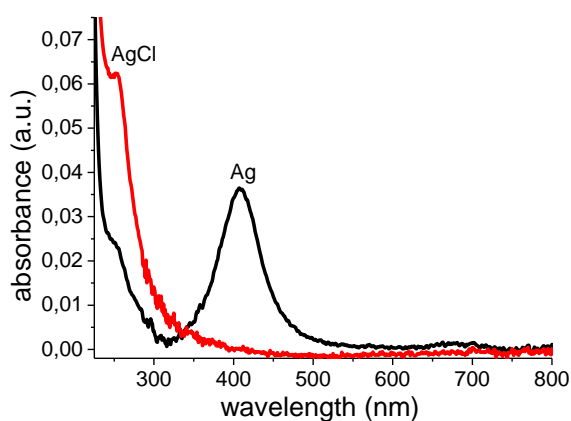
Figure 3.3 UV-Vis absorption spectra of Ag and AgCl nanoparticles by using reduction of AgNO$_3$.

When the synthesis of AgCl nanoparticles was performed at 100 ºC, silver nanoparticles completely turned into silver chloride nanoparticles. UV-vis absorption spectra (Figure 3.3) showed only characteristic absorption band of AgCl, at 252 nm.

Structural analysis was carried out by SEM. SEM image of these AgCl nanoparticles were given in Figure 3.4. This figure shows that the shape of the particles is abundantly like a cube, but at the same time, some of them are rod-like. In the SEM images, the size distribution is polydispersed. The AgCl nanoparticles under this reaction temperature exhibit irregular morphology.
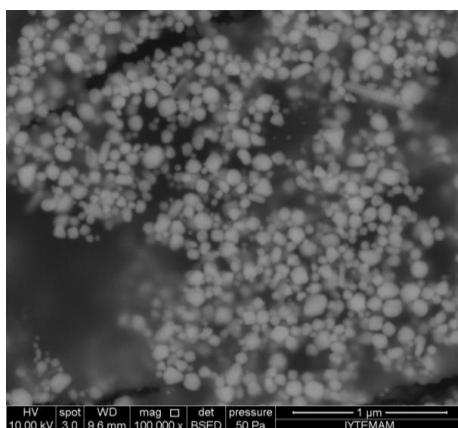
Figure 3.4. SEM image of AgCl nanoparticles synthesized at 100 ºC.

The synthesis of monodispersed AgCl nanoparticles were performed by the polyol method. Because monodispersed AgCl nanoparticles by the treatment of HCl in the aqueous phase was not obtained. Optimization studies were performed. Firstly, the ratio of $AgNO_3$ to PVP amount was varied. To do this the amount of PVP was kept constant and the concentration of $AgNO_3$ was altered as in the Table 3.1.

Table 3.1. Experimental condition of the AgCl nanoparticles by the polyol method.

PVP (M)	EG (ml)	HCl (M)	Temp (ºC)	$AgNO_3$ (M)
0.075	50	0.24	100	0.012
0.075	50	0.24	100	0.024
0.075	50	0.24	100	0.035
0.075	50	0.24	100	0.047
0.075	50	0.24	100	0.094

Figure 3.5 shows UV-vis spectra of AgCl nanoparticles synthesized by the polyol method. As the concentration of $AgNO_3$ increased from 0.012 to 0.094 M, the absorbance of the peak around 260-280 nm increased. The position of absorption peaks slightly shifted to higher wavelengths. In other words, the size of particles was supposed to be increased as illustrated at the UV-Vis spectra.
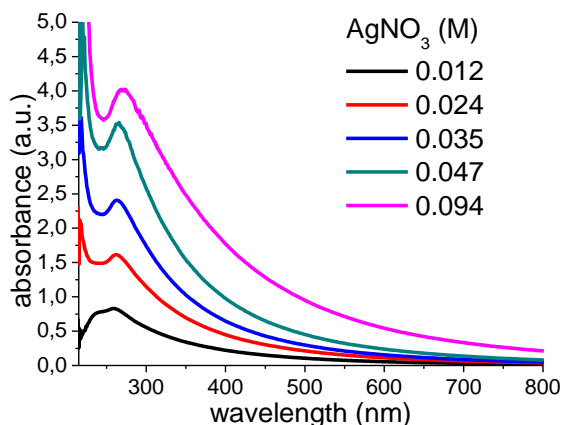
Figure 3.5. UV-vis absorption spectra of AgCl nanoparticle synthesized by the polyol method at 100ºC (the concentration of $AgNO_3$ were changed from 0.012 M to 0.094 M).

When the concentration of $AgNO_3$ was increased, the sizes of the AgCl nanoparticles were changed from 90 to 120 nm, but irregularly as shown in Figure 3.6.
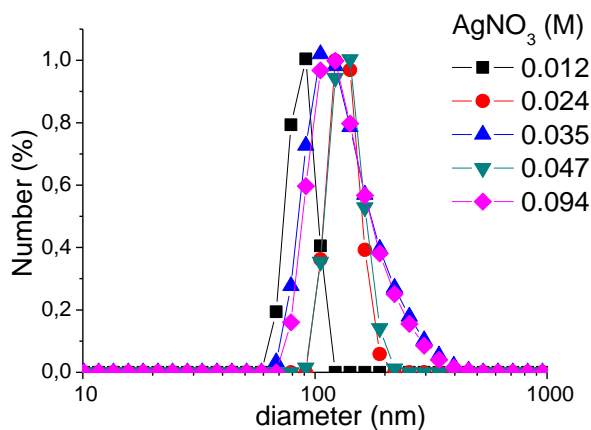
Figure 3.6. The size distribution of AgCl nanoparticles synthesized under different $AgNO_3$ concentration at 100 ºC (from 0.012 M to 0.094 M).
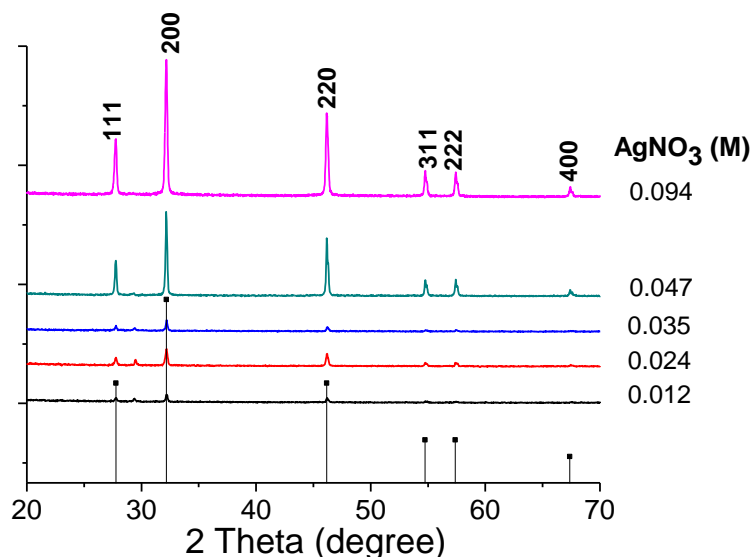
Figure 3.7. XRD pattern of AgCl nanoparticles synthesized under different $AgNO_3$ concentration at 100 ºC (from 0.012 M to 0.094 M).

XRD analysis was performed to understand the structure and the composition of the synthesized AgCl nanoparticles. Figure 3.7 shows that XRD pattern of AgCl nanoparticles synthesized under different $AgNO_3$ concentration (from 0.012 M to 0.094 M) at 100 ºC. The crystal structure of nanoparticles is rock salt (NaCl). The XRD pattern indicates when the amount of $AgNO_3$ was increased from 0.012 M to 0.094 M, the intensity of crystalline AgCl peaks increased. Figure 3.8 shows that when the concentration of $AgNO_3$ increased, the area of the XRD peaks (220) increased linearly. The number of AgCl nanoparticles increased depending on increasing the concentration of $AgNO_3$.
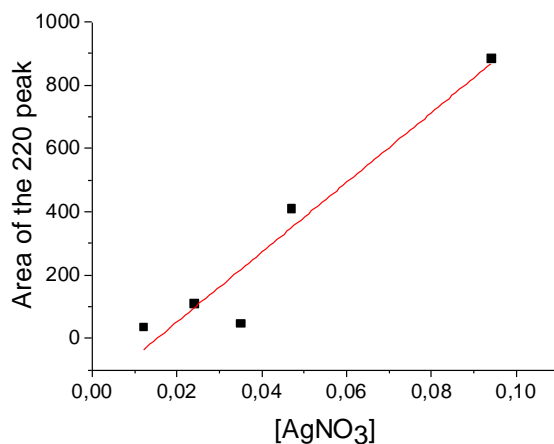
Figure 3.8. The graph of concentration of $AgNO_3$ versus the area of the XRD peak.

Figure 3.9 is the SEM images of AgCl nanoparticles, showing that the all the nanoparticles are in cubic-shape.
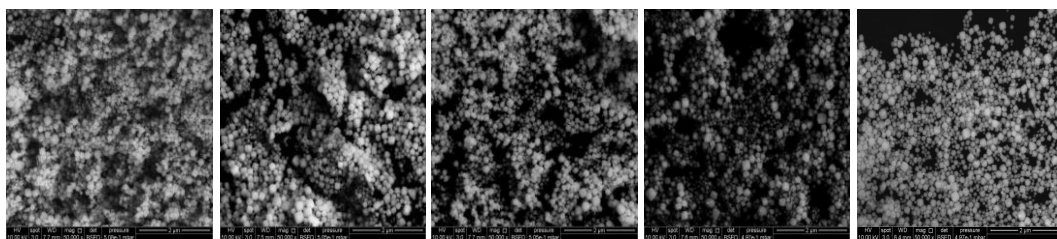
Figure 3.9. SEM images of AgCl nanoparticles synthesized under different AgNO$_3$ concentration at 100 ºC (from 0.012 M to 0.094 M (with BSED detector).

HRTEM image of AgCl nanoparticles synthesized with 0.094 M silver nitrate shows that the nanoparticles have rock salt (NaCl) structure. The HRTEM image of those particles is seen in Figure 3.10. The lattice constant of AgCl is 2.775 Å.
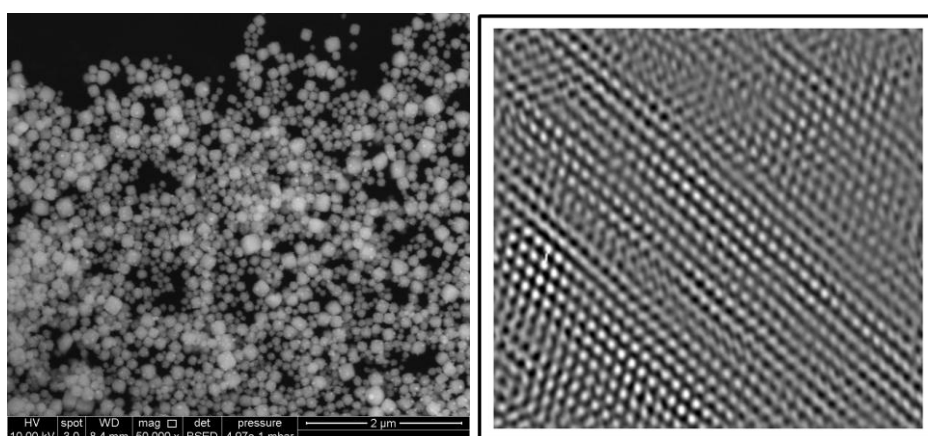
Figure 3.10. HRTEM image of AgCl nanoparticles prepared by the polyol method.

After determining the appropriate concentration of silver nitrate, the concentrations of all reactants were halved as in the Table 3.3.

When the total concentration in the medium reduced by half, there was no a major change in the size and shape of the nanoparticles. Figure 3.11 shows that morphology of AgCl nanoparticles is still cubic and size of the particle is approximately 100 nm. Also according to EDS result particles are AgCl nanoparticles. Thus, lower amount of AgNO$_3$ allowed us to obtain of AgCl nanoparticles with the same properties as they were obtained at higher concentration of AgNO$_3$. We used the formulation given below (Liu et al. 2007).

$$N = \frac{\pi}{6} \, \rho \, \frac{D^3}{M} \, N_A \quad \text{and} \quad C = \frac{N_{Total}}{N \, V N_A} \tag{3.1}$$

Where N is the number of atoms per nanoparticle, ρ is the density of halite silver chloride, D is the average diameter of nanoparticles, M is the atomic mass of silver chloride, N_A is the number of atoms per mole, V is the volume of the reaction solution. By taking the D is 100 nm (DLS measurement), ρ is 5.56×10^{-21} g/nm^3, M is 143.32 g/mol, N_A is 6.022×10^{23} atoms/mol and V is 50 ml. We calculated the number of silver chloride atoms per particle (N) and the number of silver chloride particles per cm^3 as follows:

Table 3.2. Calculation of the number of particles per cm^3

Size (nm)	N (the number of AgCl atoms per particle)	C (the number of AgCl particles per cm^3)
100 nm	12.0×10^6 atoms/NP	2.3×10^{12} NP/cm^3

Table 3.3. Experimental condition of changing the total concentration of $AgNO_3$.

EG (ml)	Temp (ºC)	$AgNO_3$ (M)	PVP (M)	HCl (M)
50	100	0.094	0.0750	0.24
50	100	0.047	0.0375	0.12
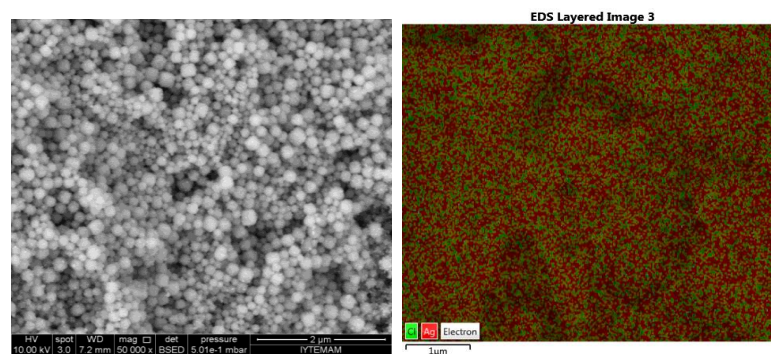
Figure 3.11. SEM image and EDS mapping AgCl nanoparticles synthesised with halved concentration of $AgNO_3$.

For constant reactant concentrations, the reaction temperature was changed from 20 to 150 ℃. Table 3.3 shows the concentration of the reactants and the temperature of the reaction.

Table 3.4. The concentration of the reactants and the temperature of the reaction.

AgNO$_3$ (M)	PVP (M)	EG (ml)	HCl (M)	Temp (℃)
0.047	0.0375	50	0.12	20
0.047	0.0375	50	0.12	60
0.047	0.0375	50	0.12	100
0.047	0.0375	50	0.12	120
0.047	0.0375	50	0.12	140
0.047	0.0375	50	0.12	150

Figure 3.12 indicates both the absorption spectra of Ag nanoparticles and of AgCl nanoparticles which were prepared after adding HCl to the Ag nanoparticle dispersion. According to this figure, when HCl was added to the Ag nanoparticles dispersion, the absorption peak of Ag nanoparticle which appeared at 408 nm disappeared and the absorption peak of AgCl become visible. Although the absorption peak of AgCl nanoparticles at 20 ℃ was at 254 nm, the peak was shifted to 350 nm when the AgCl nanoparticles were synthesized at 140 ℃. At 150 ℃, two peaks were observed at 278 nm and 430 nm. 278 nm is the absorption peak of AgCl nanoparticles, but 430 nm belongs to Ag nanoparticles. The shift is due to the increase in size of the nanoparticles until 140 ℃. A new nanoparticles (AgCl:Ag) were obtained at 150 ℃. The size distribution of the nanoparticles is shown in Figure 3.12.
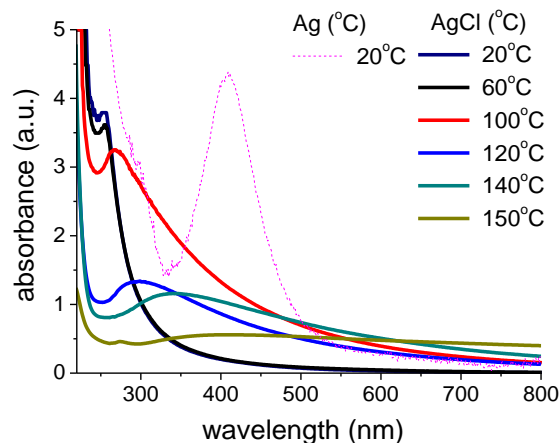
Figure 3.12. UV-vis absorption spectra of Ag nanoparticles and AgCl nanoparticles synthesized at different reaction temperatures.

The average size and this distribution of the AgCl nanoparticles were measured by DLS measurement. When Ag nanoparticles were synthesized at the room temperature, the size of these nanoparticles was 60±11 nm. However, AgCl nanoparticles at room temperature were 68±12 nm. When the temperature of the reaction was increased to 100 ℃, the size of the AgCl nanoparticle was increased to 100±34 nm. The size of the AgCl:Ag particle size was reached up to 692±180 nm under the synthesis of 150 ℃.
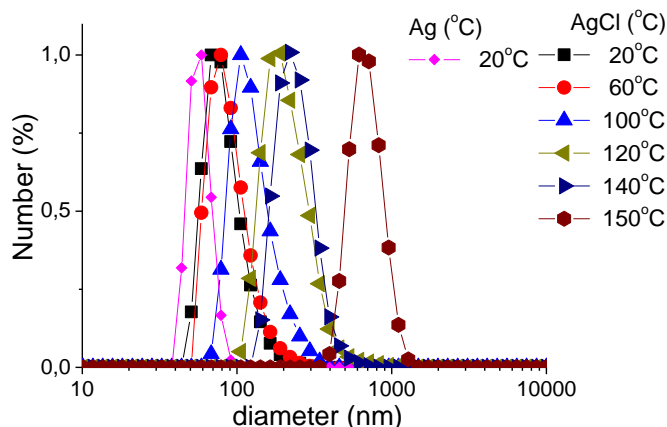
Figure 3.13. Size distribution of AgCl nanoparticles synthesized at different temperature.

The SEM images seen in Figure 3.14 show that the AgCl nanoparticles formation started at 60 ℃, but the shape of the nanoparticles was not totally cubes. However, when the reaction temperature was increased to 100 ℃, the shape of particles

was dominantly cube and the size distribution of the particles synthesized at 100 ℃ was better than that of the particles obtained at 60 ℃. If the temperature was increased over 100 ℃ (like 120-140-150 ℃), the shape and type of nanoparticle was started to change as shown in the Figure 3.13.
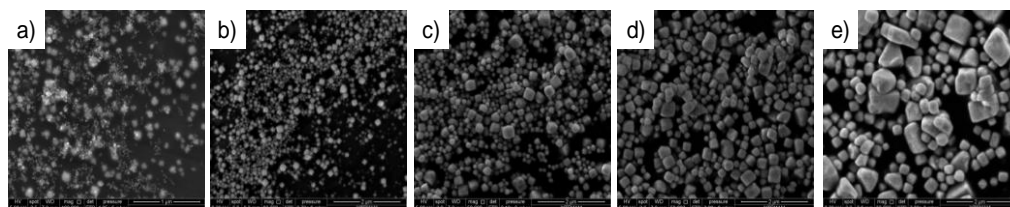
Figure 3.14. SEM images of AgCl nanoparticle at synthesized at different reaction temperature. a) 60 ℃, b) 100 ℃, c) 120 ℃, d) 140 ℃, e) 150 ℃

Figure 3.15 shows that SEM images of synthesized AgCl nanocubes at 100 ℃ with ET and BSE detector. The principle of BSE detector is strongly related to the atomic number (Z) of the specimen. In other words, if greater average Z as Ag is in the sample, a "brighter" SEM image is taken. Therefore, the SEM image of AgCl nanoparticles by using BSE detector is better and clearer than the ET detector.
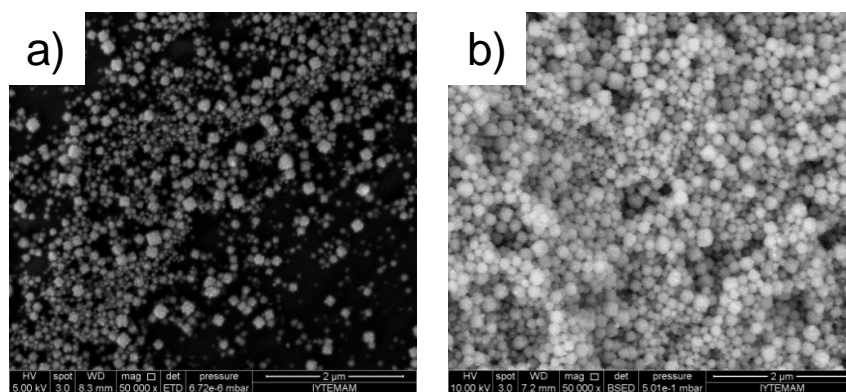
Figure 3.15. SEM image of AgCl nanocubes at 100 ℃. a) with ET detector, b) BSE detector

Figure 3.16. shows that when the reaction temperature was increased to 150 ℃, Ag nanoparticles formed at the corners of the AgCl nanocubes and, therefore AgCl:Ag nanoparticles were obtained.
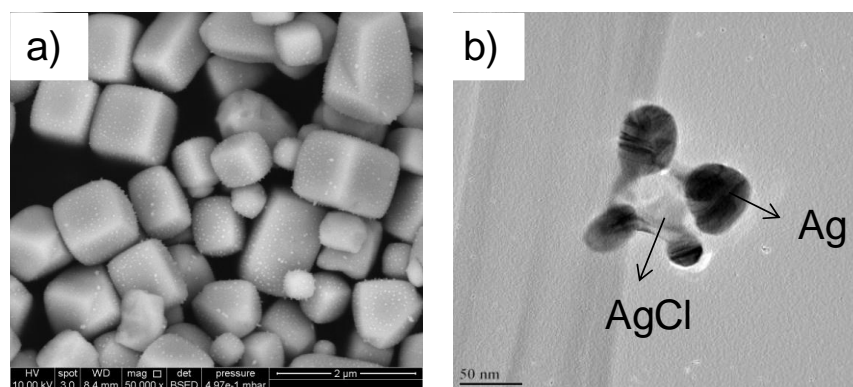
Figure 3.16. a) SEM and b) HRTEM image of AgCl nanocubes at 150 ℃.

Figure 3.17 illustrates that XRD pattern of the synthesized nanoparticles at 100 ℃ and 150 ℃. The XRD pattern at 100 ℃ shows the presence of crystal structure of the AgCl nanoparticles, but both Ag and AgCl crystal structures were observed at 150 ℃.
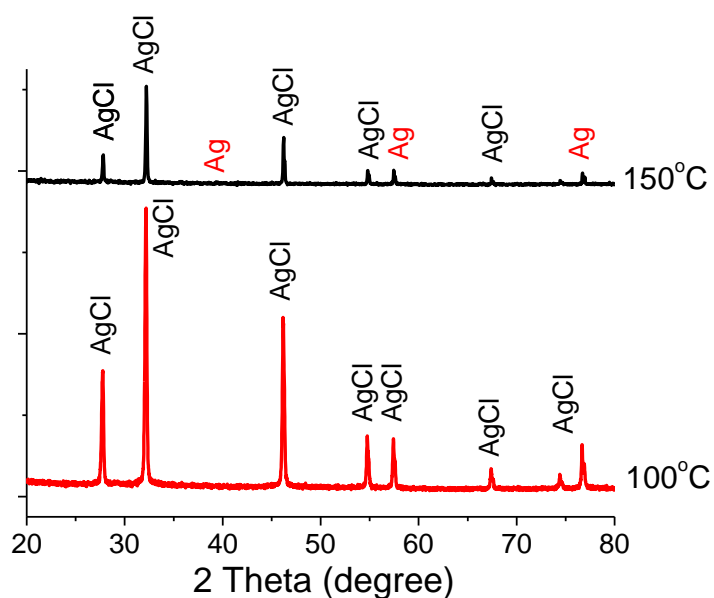
Figure 3.17. XRD patterns of the synthesized AgCl and AgCl:Ag nanoparticles at 100 ℃ and 150 ℃, respectively.

To see the effect of HCl concentration on the particle morphology and size, the concentration of HCl was changed.The concentrations of silver nitrate and PVP were respectively chosen as 0.047 M and 0.0375 M PVP with a fixed reaction temperature were fixed at 100 ℃. The change in the HCl concentration is given in Table 3.4.

Table 3.5. The change in the HCl concentration

AgNO$_3$ (M)	PVP (M)	EG (ml)	Temp (ºC)	HCl (M)
0.047	0.0375	50	100	0.120
0.047	0.0375	50	100	0.050
0.047	0.0375	50	100	0.012
0.047	0.0375	50	100	0.005

Under low concentrations of HCl, the synthesis of AgCl nanoparticles was not possible. Figure 3.18 confirms that, the white color was not observed because AgCl nanoparticles were not synthesized when the concentration of HCl was not sufficient. The pink color was observed in the reaction solution due to AgCl nanoparticles were not formed. The UV-Vis spectra show that there is no characteristic peak of AgCl nanoparticle. AgCl nanoparticles were not formed in the presence of lower concentration of HCl solution. When the concentration of HCl was 0.12 M, the synthesis of AgCl nanoparticles was achieved. The characteristic absorption peak of the AgCl nanoparticles was appereared at 265 nm, as shown in Figure 3.16.

Figure 3.18. Synthesis of AgCl nanoparticles changing the concentration of HCl.
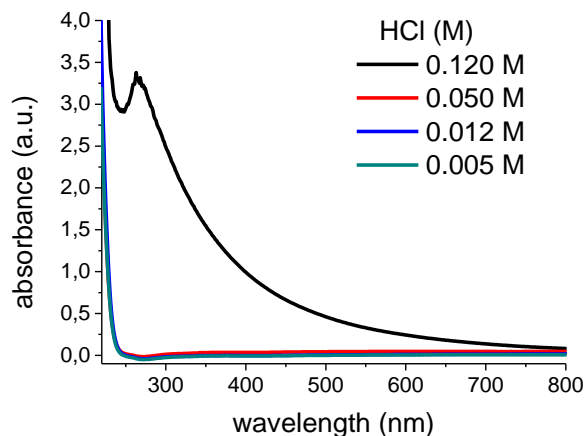
Figure 3.19. UV-vis absorption spectra of AgCl nanoparticles synthesized under different HCl concentrations.

Figure 3.20 indicates that the effect of the concentration of HCl on the particle morphology. When the concentration of HCl was so small, AgCl nanoparticles were not observed in Figure 3.20.a and Figure 3.20.b. However increasing the concentration of HCl to fix $AgNO_3$:HCl is equal to 1:1, even if the image was bad in general, the SEM image of this sample included some nanoparticles like cubic shape in Figure 3.20.c. When the concentration of HCl is 2.5 times higher than the concentration of $AgNO_3$, AgCl nanocubes were formed perfectly. According to these results, the ideal concentration of HCl is 0.120 M for this study.
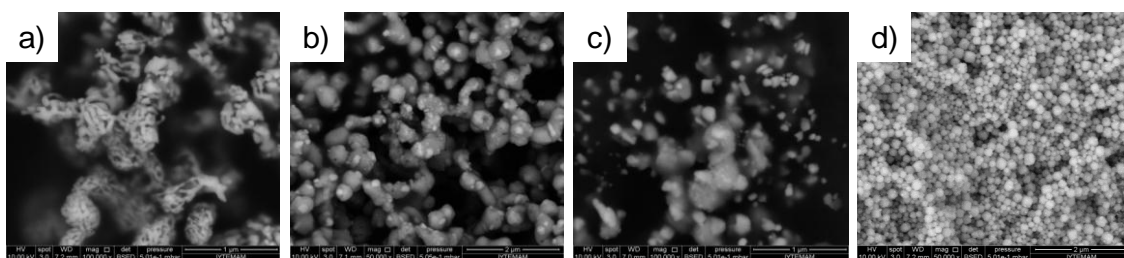
Figure 3.20. SEM images of AgCl nanoparticles at synthesized at different concentration of HCl. a) 0.005 M ($AgNO_3$:HCl = 1:0.1), b) 0.012 M ($AgNO_3$:HCl = 1:0.25), c) 0.050 M ($AgNO_3$:HCl = 1:1), d) 0.120 M ($AgNO_3$:HCl = 1:2.5)

3.4. Discussion

As shown in Figure 3.3 and Figure 3.4, when HCl was added to the synthesized Ag nanoparticles, the shape of the particles was irregular and the size distribution was polydispersed. Therefore, the polyol method was prefered to obtain monodispersed AgCl nanoparticles. In this work, how $AgNO_3$ amounts, the reaction temperature and HCl concentrations were affected on the size and the shape of AgCl nanoparticles.

Effect of AgNO$_3$: When the concentration of $AgNO_3$ was increased from 0.012 M to 0.094 M, narrower exciton absorption peaks of AgCl nanoparticles were observed, because exciton energy levels. The excitonic peak maximum was shifted towards higher wavelength with increasing $AgNO_3$ concentration from 0.012 M to 0.094 M due to size effect. When AgCl nanoparticles were synthesized by using 0.094 M $AgNO_3$, the exciton absorption band was observed at higher wavelength. The small band gap energy was observed for these AgCl nanoparticles. The conductivity of these nanoparticles was higher than the AgCl nanoparticles which were synthesized by using 0.012 M $AgNO_3$ because the conductivity of semiconductors is strongly dependent on the band gap (Rao et al. 2002).

Effect of Temperature: The reaction temperature was increased from 20 ºC to 150 ºC, when the concentrations of reactants were kept constants. Following the addition of HCl on the Ag nanoparticles, the typical absorption peak of AgCl was observed until 150 ºC. The peaks shifted to red depending on the size effect, because the optical properties of semiconductor are sensitive to the crystal size. According to Uv-Vis absorption spectra and HRTEM image at 150 ºC morphology of the particles changed to AgCl:Ag nanoparticles. Ag nanoparticles are formed on the AgCl nanocubes when the temperature is increased to 150 ºC due to enhancing reducing feature of ethylene glycol (Peng and Sun 2011). The ethylene glycol is converted to acetaldehyde which reduces Ag^+ to Ag^o (Zhu et al. 2011).

$$2\ HOCH_2CH_2OH \longrightarrow 2CH_3CHO + 2H_2O \qquad (3.2)$$

$$2Ag^+ + 2CH_3CHO \longrightarrow CH_3CHO\text{-}OHCCH_3 + 2Ag^o + 2H^+ \qquad (3.3)$$

At high temperature AgCl nanoparticles converted to Ag nanoparticles partially. Therefore, the bands at 278 nm of the absorption spectra given in Figure 3.12 present the characteristic excitonic band of the AgCl nanoparticles. The band at 430 nm belongs to the Ag nanoparticles.

SEM images of the nanoparticles are shown in Figure 3.14. The change in shape of the particle was observed after 130 ºC. The reason is that the boiling point of PVP is 130 ºC. At 140 ºC and 150 ºC, PVP boiled completely, and the particle shape was transformed to from cubic form. Therefore, it indicates that the presence of PVP plays important role on the particle shape and size.

Effect of HCl concentration: Kim and coworkers studied the effect of HCl concentration on the morphology at 150 ºC (Kim et al. 2010). They reported that if the HCl concentration is smaller than the $AgNO_3$, the AgCl nanowires are started to appear. When the ratio of $AgNO_3$ and HCl is increased to 1:2, cubic AgCl nanoparticles are started to observe. They demonstrated that this ratio is increased to 1:4 and 1:6, the perfectly cube AgCl nanoparticles are observed. Therefore, we studied different molar ratios of $AgNO_3$ and HCl such as 1:2.5; 1:1; 1:0.25 and 1:0.1 in order to show effect of HCl concentration on the morphology. According to the SEM image of these samples, we confirmed that the morphology of the nanoparticles is affected highly. Unlike the study of Kim and coworkers, we obtained perfectly AgCl nanocube, when the ratio of $AgNO_3$ and HCl was 1:2.5. Also, the size of our AgCl nanocubes is the 100 nm because our reaction temperature is lower than the study of Kim et al. Shortly, we can say that the concentration of HCl should higher than the $AgNO_3$ concentration to form perfect AgCl nanocube.

3.5. Conclusion

Silver chloride nanocubes were synthesized with two different methods. First, HCl was added to prepared silver nanoparticles in the aqueous phase. However, the shape and size of these particles were not homogenous and monodispersed, respectively. Then, silver chloride nanoparticles were synthesized by the polyol method. Cube-shaped AgCl nanoparticles were prepared by the reaction between Ag nanoparticles and HCl at 100 ºC. HCl was used as Cl^- source in this method. The effect of molarity of silver source, molarity of Cl^- source and the effect of reaction temperature

on the morphology and size of the nanoparticles were studied. We determined the optimum concentrations. The concentration of silver nitrate, PVP and HCl were respectively determined as 0.047 M, 0.0375 M and 0.12 M. The optimum reaction temperature was determined to be 100 ºC to obtain monodispersed and single shaped AgCl nanocubes.

CHAPTER 4

A NOVEL COMPOSITE CONTAINING AgCl NANOPARTICLES and POLYANILINE for DEVELOPMENT of ECG SENSOR

4.1. Introduction

Bioelectric signals are come into existence during the activities of human body neural system and muscle of various organs such as brain and heart. The basis of bioelectric signals generates an action potential, which is the potential difference between the internal and external sides of the cell membrane, as a result of electrochemical events in cells (Khandpur 2005). The typical signal magnitude is of a few microvolts. Electric potentials on the surface of living tissues are measured by the electrocardiography (ECG), electromyography (EMG) and electroencephalography (EEG) systems. These biopotential recordings are very important to understand the physicochemical and physiological processes in the living systems (Neuman 2001a).

Electrocardiography (ECG) is the measure of the electric activity of the heart and is used in diagnosing disturbances in the cardiac rthym, and detecting any irregularities that may occur in the circulatory system (GHANI 2008). The electric activity of heart cell is defined with the ion exchange sodium (Na^+), potassium (K^+) and chloride (Cl^-) through the cell membrane (Robert Plonsey 2007).
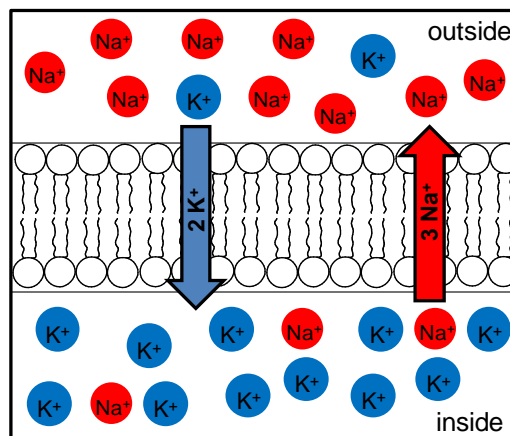
Figure 4.1. ion-exchange in the cell

The generated ionic current flow in the body can be measured with the biopotential electrodes. A biopotential electrode provides measuring the electric potential on the surface of skin and acts as a transducer in order to convert ionic current to electron current. The conversion process of ion current to electron current proceeds at the electrode-electrolyte interface (Neuman 2000).

Electrons as a current-carrier are found at the interface side of the electrode and the cations (C^+) and anions (A^-) are found at the interface side of the electrolyte. To provide a charge transfer from the electrode to the electrolyte or the reverse direction needs an oxidation-reduction reaction between the metal and the ionic solution as seen in the equations shown below (Yazicioglu 2009).

$$C \rightleftarrows C^{n+} + ne^- \tag{4.1}$$

$$A^{m+} \rightleftarrows A + me^- \tag{4.2}$$

As a result of this reaction, free electrons come out in the electrode. Hence, the current pass from the electrode to the electrolyte.
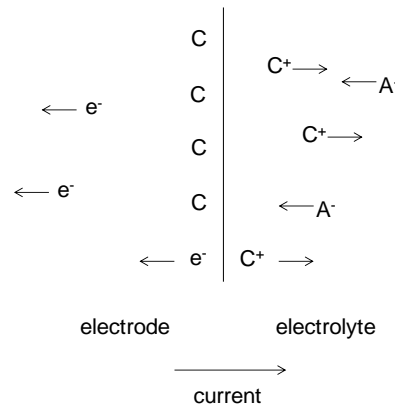
Figure 4.2. Electrode-Electrolyte Interface
(Source: Neuman 2001b)

Theoretically, the electrodes can be polarized or non-polarized (Neuman 2001a). The current transition is limited at the electrode-electrolyte interface of the polarized electrodes. Also, these electrodes behave as a capacitor. However, current passes freely across the electrode-electrolyte interface of the non-polarized electrodes and they act as *a resistor*. Ag/AgCl (silver/silver chloride) electrode is known as a non-polarized electrode. Ag/AgCl electrodes have low impedance because of presence of

AgCl layer. Half-cell potential of these electrodes (approximately 220 mV) is very stable, in other words they have very low noise. In addition, fabrication of these electrodes is easy and inexpensive (Neuman 2000).

In this study, it was aimed to develop a AgCl/polyaniline (PANI) nanocomposite for a fabrication of ECG electrodes. AgCl nanoparticles were preferred to use due to their easy and inexpensive fabrication. They have low impedance and their half cell potential is small. PANI was used as a bridge between the ABS (Acrylonitrile Butadiene Styrene) and AgCl nanoparticles. PANI has unique properties such as exhibiting good ambient stability, wide and controllable range of conductivity and providing low cost solutions for the coating process. These properties allow them to be used in different application areas such as energy storage, energy transportation, organic electrodes and sensors etc.

4.2. Experimental

ECG electrode materials, AgCl nanoparticles and PANI were developed in this work.

4.2.1. Reagents

Metal source; silver nitrate (99%) ($AgNO_3$), ammonium persulfate (APS) (98%) and HCl (37%) were purchased from Sigma-Aldrich. Poly(vinylpyrolidone) (PVP) (M.W.$\approx$ 8,000) were bought from Alfa-Easer. Aniline was purchased from Merck. Deionized (DI) water was used throughout the study.

4.2.2. Cleaning the surface of ABS (Acrylonitrile Butadiene Styrene) before the coating

Surface cleanliness of the ABS is very important for coating. Surface to be coated must be clean because the dirty surface (containing dirt and oil molecules) may cause inhomogeneous coating of the nanoparticles on the applied surface. Therefore, three different methods were used in order to find out the best cleaning approach. The methods were

1) Ultrasonic bath,
2) Chemical method,
3) Ozone cleaner.

In ultrasonic bath method; ABS substrate was cleaned with the solutions of different percentages of water and acetone under sonication for 5 -15 min. The contact angle of ABS was measured 80 ° by using the drop shape method. Table 4.1 indicates the percentage of cleaning solution and the results of contact angle measurements of ABS. The best purification (cleaning) in other words the lowest contact angle was obtained with solution of 25% water-75% acetone mixture under 5 min sonication.

Table 4.1. Contact angles after cleaning with ultrasonic bath

Contact angles after cleaning with ultrasonic bath			
	5 min	**10 min**	**15 min**
100% water	78º	75º	73º
75% water - 25% acetone	75º	70º	65º
50% water - 50% acetone	66º	64º	65º
25% water - 75% acetone	59º	dissolved	dissolved
100% acetone	dissolved	dissolved	dissolved

In chemical method for cleaning (purification); five basic steps were followed. They were;

1)   Cleaning of ABS with aqueous solution of 1.0 M NaOH and 0.07 M
        Na_2CO_3 at two different temperatures (20 ºC and 60 ºC) for 5 minutes.
2)   Rinsing with deionized water for 3 minutes
3)   10% HNO_3 solution for 30 seconds
4)   Rinsing with cold water for 3 minutes
5)   Rinsing with hot water (60 ºC) for 5 minutes

After cleaning of ABS via the chemical method, contact angle measurements were done. Table 4.1 shows the results of the measurements, but there were differences

in the contact angles. That's why this method is not proper because results are not repeatable.

Table 4.2. Contact angles after cleaning with chemical method

Contact angles after cleaning with chemical method		
	20ºC	**60ºC**
1st	44º	35º
2nd	50º	43º
3rd	44º	55º

The plasma cleaning (ozone cleaning); O_2 plasma was created by using high frequency voltages to ionize the O_2-air mixtures and it was used to remove impurities and contaminants from the ABS surface. In Table 4.3 , the contact angle measurements of ABS were tabulated. The contact angle decreased from 80 ºC to approximately 25 ºC, thus the surface of ABS was became hydrophilic. The best cleaning results were obtained with the O_2 plasma cleaner.

Table 4.3. Contact angles after cleaning with O_2 plasma cleaner

Contact angles after cleaning with O_2 plasma cleaner	
1st	22°
2nd	22°
3rd	25°
4th	30°
5th	30°

4.2.3. Coating Procedures of ABS Substrate to Fabricate ECG Electrode

A. Mixing Method

ABS (Acrylonitrile Butadiene Styrene) which is the support material of ECG electrode was coated with the AgCl nanoparticles. Synthesis and the characterization of the AgCl nanoparticles were explained in the chapter 3. After cleaning the ABS, the purified AgCl nanoparticles were redispersed in water and mixed with the ABS substrate.

B. Adding AgCl Nanoparticles during Aniline Polymerization on the ABS Surface

After cleaning the ABS substrate, ABS surface was coated with polyaniline by using simple chemical polymerization. Synthesized AgCl nanoparticles in chapter 3 were added to reaction medium during the polymerization.

C. Simultaneous Polymerization and AgCl Nanoparticle Formation on ABS Surface

The support material (ABS) was coated by conducting polyaniline containing AgCl nanoparticles, deposited on the surface of ABS by using simple chemical polymerization.

Coating processes took place in two-steps.

1) ABS polymer substrates were mixed with 10% aniline solution containing 0.1 M $AgNO_3$ and 0.1 M PVP for 5 min. This provided adsorption of aniline and Ag nanoparticles on the surface of ABS. Then, these substrates were washed with flowing water.

2) After washing, substrates were stirred in a solution of 0.5 M ammonium persulfate, 0.4 M HCl and water for 20 min to polymerize the aniline to the polyaniline and to convert Ag nanoparticles to AgCl nanoparticles. Finally,

these substrates were purified with water and allowed to dry under vacuum during 24 h at room temperature.

4.3. Results

Coating of ABS Substrate: After the cleaning process, ABS was tried to be coated with the AgCl nanoparticles. Figure 4.3 shows the pictures of coated ABS. AgCl nanocubes were adsorbed on the ABS surface, but the conductivity could not been measured on the surface of ABS. Coating thickness was very thin therefore the coated layer of AgCl was easily removed on the surface of ABS.

Figure 4.3. Coating of the ABS with the AgCl nanocubes

Due to this ineffective coating procedure, a new method was needed to perform for permanent coating. Polyaniline was used to adsorb AgCl nanocubes on the surface of the ABS. PANI was preferred because it can be synthesized easily and it is stable under the environmental factors. Taking advantage of this knowledge, simple polymerization method was developed to polymerize aniline on the surface of the ABS. The process took place on two-stages. The first step is mixing aqueous solutions of aniline and ABS substrate at room temperature. Then, the ABS substrate which was functionalized with aniline was mixed with ammonium peroxydisulfate solution in acidic medium at room temperature under the atmospheric pressure. Ammonium peroxydisulfate oxidizes aniline because it initiates radical formation.

Interaction of aniline and ABS matrix was beneficial for the deposition of conductive polyaniline on the surface of ABS. Figure 4.4 shows the proposed mechanism for aniline polymerization on the ABS surface. The amine group of aniline

attacts to the most reactive C atoms of C≡N group in the ABS structure. After aniline interacts with the ABS, C=N turned to C=O bond in the aqueous phase, due to the acidity depending on HCl. After in the step 4 resonance structure occurred, ammonium peroxydisulfate attacts to H to form radical. Figure 4.4 shows intiation of radical formation by ammonium peroxydisulfate in the medium. Oxidized aniline started radical chain polymerization to obtain polyaniline on the ABS surface. Polymerization goes on by repeating similar reaction in the medium.

PANI on the ABS surface
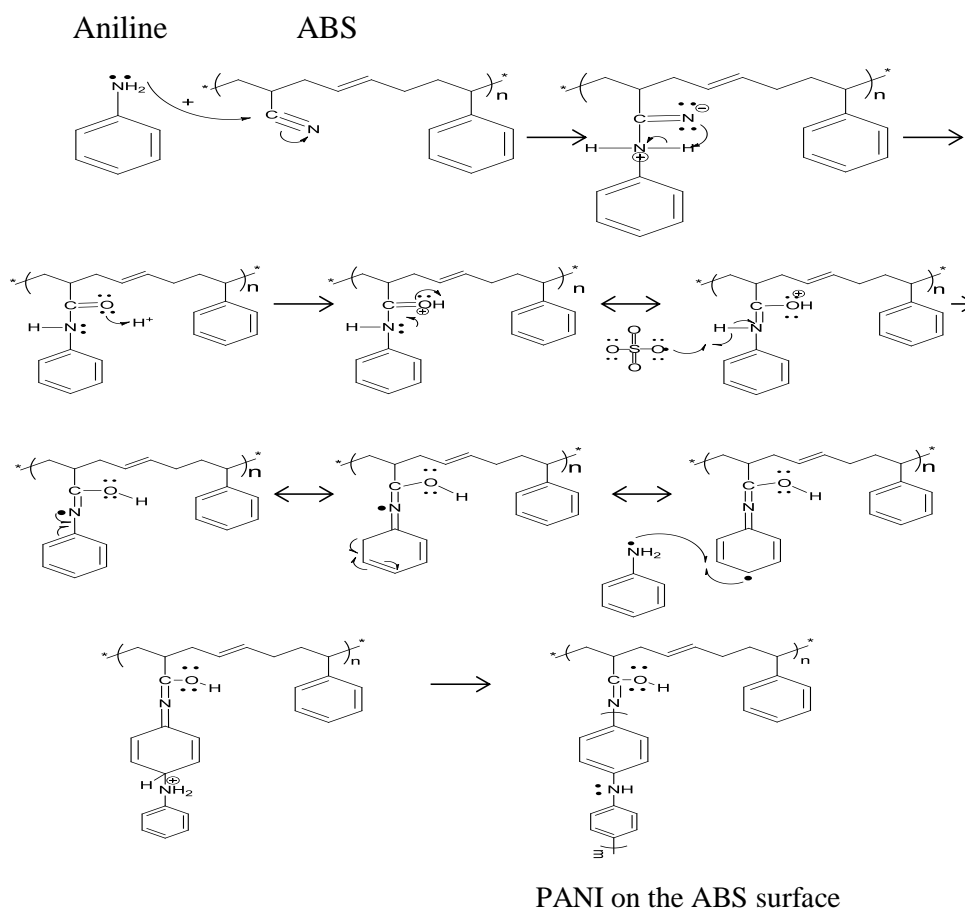
Figure 4.4. The proposed mechanism for aniline polymerization on the ABS surface.

Figure 4.5 shows that SEM-EDS image of the coated ABS surface with polyaniline and EDS analysis. The EDS-mapping confirmed that, the surface of ABS was completely coated with polyaniline. Resistance of this coated ABS was measured with a voltmeter and found that 2.67±0.2 kΩ. Although the surface of ABS was coated homogeneous with the polyaniline with having conductivity, however ECG signal was not obtained with this electrode. The most probable reason for this situation may be the

electrode which was prepared with polyaniline. ''only'' is not providing ionic transport. The electrode could not act like a transducer that converts ionic current to electron current. Hence, AgCl nanocubes were added to the medium during the polymerization step in order to being to convert ion of ionic current to electron current.

Element	Wt%	Atomic%
C	26.87	32.84
N	0.40	0.42
O	72.73	66.74
Total:	100.00	100.00
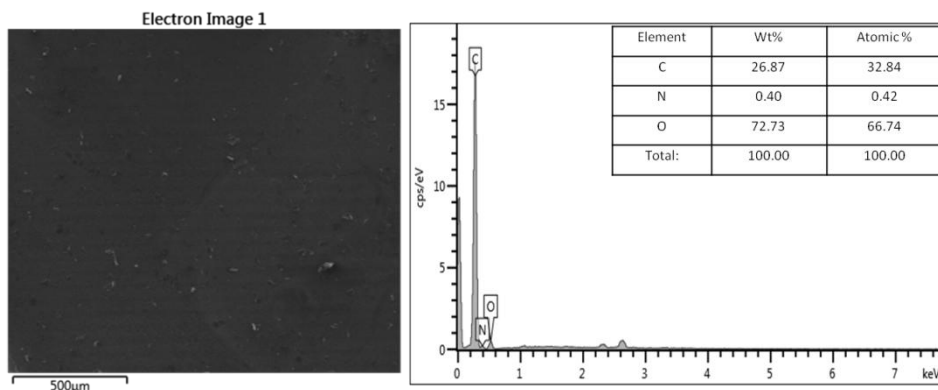
Figure 4.5. SEM image and SEM-EDS mapping of the coated ABS surface with polyaniline.

After purifying the AgCl nanocubes whose synthesis was explained in chapter 3, they were re-dispersed in ethylene glycol and, added in the first step of the polymerization. However, polyaniline was not doped by these nanocubes. Moreover, purified AgCl nanocubes were redispersed in the mixture of ethylene glycol and water having various proportions. Figure 4.6 shows the SEM images and EDS results of the polyaniline coated ABS surface. Polyaniline was doped with the AgCl nanocubes. These AgCl nanocubes were synthesized in chapter 3. After purification, they re-dispersed in different proportions of ethylene glycol and water mixtures and then they added to polymerization of aniline. In Figure 4.6.a, SEM images of coated ABS with PANI and AgCl nanocubes composite are seen. After purification, AgCl nanocubes were re-dispersed in 25% EG-75% water mixture. 2 ml of this dispersion were added to the first step of polymerization of aniline process. However, according to EDS results shown in Figure 4.6.a, amount of Ag (0.03 wt%) and Cl (0.39 wt%) were very low on the ABS surface. But when the percentage of ethylene glycol was increased to 50%, Ag (0.29 wt%) and Cl (2.80 wt%) percentage increased sligthly in Figure 4.6.b. Figure 4.6.c indicates that when the percentage of ethylene glycol was increased to 75%, the percentage of Ag and Cl was determines as 0.98 wt% and 1.02 wt%, respectively.
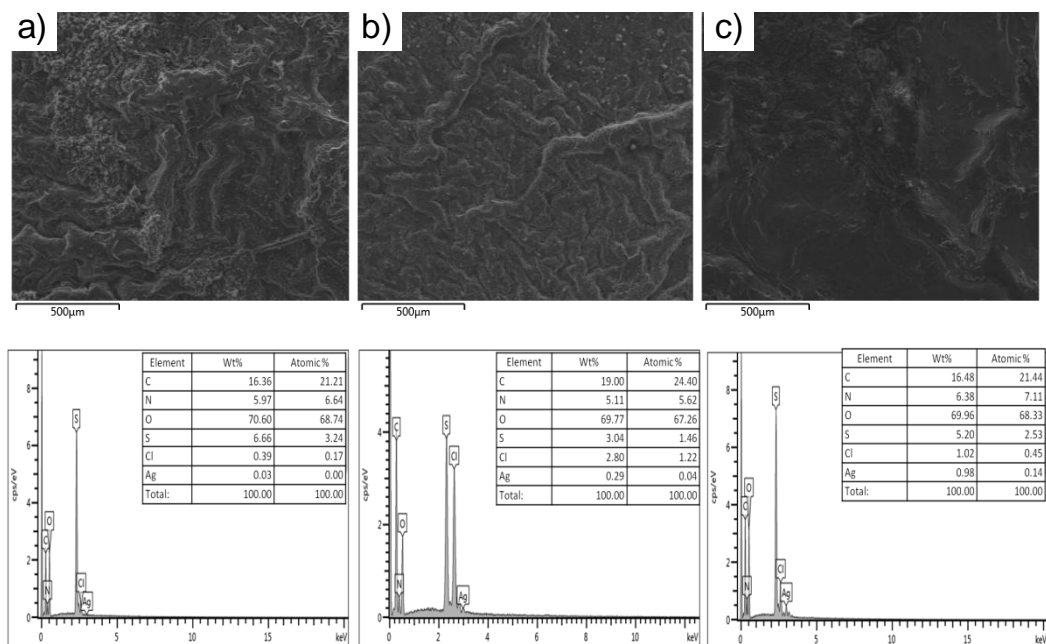
Figure 4.6. SEM images and EDS results of coated ABS with a) PANI/AgCl nanocubes (AgCl NCs were dispersed in 25% EG-75% water), b) PANI/AgCl nanocubes (AgCl NCs were dispersed in 50% EG-50% water), c) PANI/AgCl nanocubes (AgCl NCs were dispersed in 75% EG-25% water)

After the coating process, resistivity of the surface was measured by using a voltmeter. Table 4.4 indicates that, the resistivity of sensor was 2.67 kΩ. However, on the coated surface increasing the amount of AgCl, the resistivity of sensor decreased from 2.67 to 1.83 kΩ. In other words, the conductivity of the ABS surface increased approximately by one and half due to increasing amounts of AgCl on the surface.

Table 4.4. Change in resistance depending on the percentages of Ag and Cl amount

	Ag (wt%)	Cl (wt%)	Resistance (kΩ)
Only PANI	0	0	2.67
PANI+AgCl NCs (AgCl NCs were dispersed in 25% EG-75% water)	0.03	0.39	2.40
PANI+AgCl NCs (AgCl NCs were dispersed in 50% EG-50% water)	0.29	2.8	2.12
PANI+AgCl NCs (AgCl NCs were dispersed in 75% EG-25% water)	0.98	1.02	1.83

a)   b)
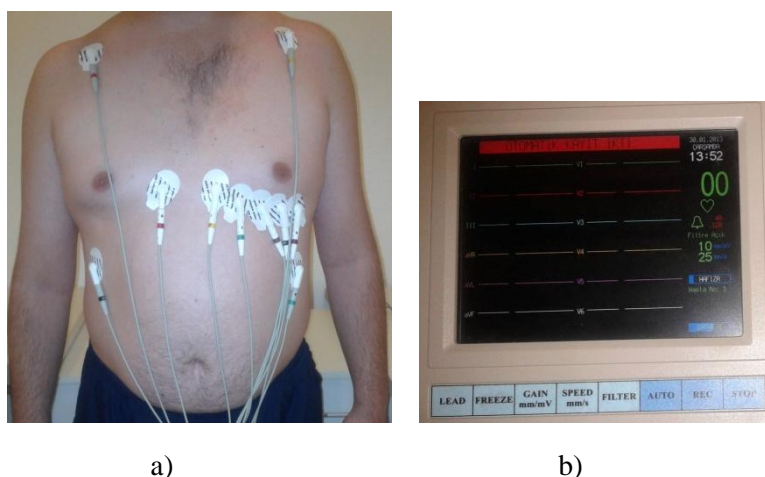
Figure 4.7. (a) Implementation of ECG measurement with coated ABS electrode with polyaniline and AgCl nanoparticles on a human body and (b) ECG graph

Even though, impedance of the electrode decreased after the addition of AgCl nanocubes, no ECG signals was observed (Figure 4.7.b) indicating that lower amount of AgCl nanocubes on the electrode surface.

Since no ECG signal was observed in the presence of AgCl nanoparticles on the PANI coated ABS, a new method for the preparation of the electrode was developed. Two considerations were important for the development. The first one was the aniline polymerization on the surface of ABS. The polymerization was conducted based on the formation of cation radicals to initiate the reaction (Patil, Matveeva, and Parkhutik

2002). The second consideration was the preparation of the Ag/PANI nanocomposite during the polymerization (Y. B. Wankhede 2013b). PANI and AgCl nanoparticle were simultaneously synthesized on the surface of ABS.

Figure 4.8 shows SEM images and the results of EDS analysis for ECG electrode prepared by the new method. Figure 4.8.a shows the picture of the fabricated ECG sensors. Figure 4.8.b is the image of the surface of the sensor. This image shows that the ABS surface was homogeneously coated with the composite material (PANI/AgCl NP). Figure 4.8.c. illustrates that the AgCl nanoparticles are rod-shaped. The EDS analysis shows the ratio of atomic percentage of Ag to Cl is 1.15 (Figure 4.8.d).

Element	Wt%	Atomic%
C	20.23	46.90
N	14.36	28.54
Cl	14.55	11.43
Ag	50.86	13.13
Total:	100.00	100.00
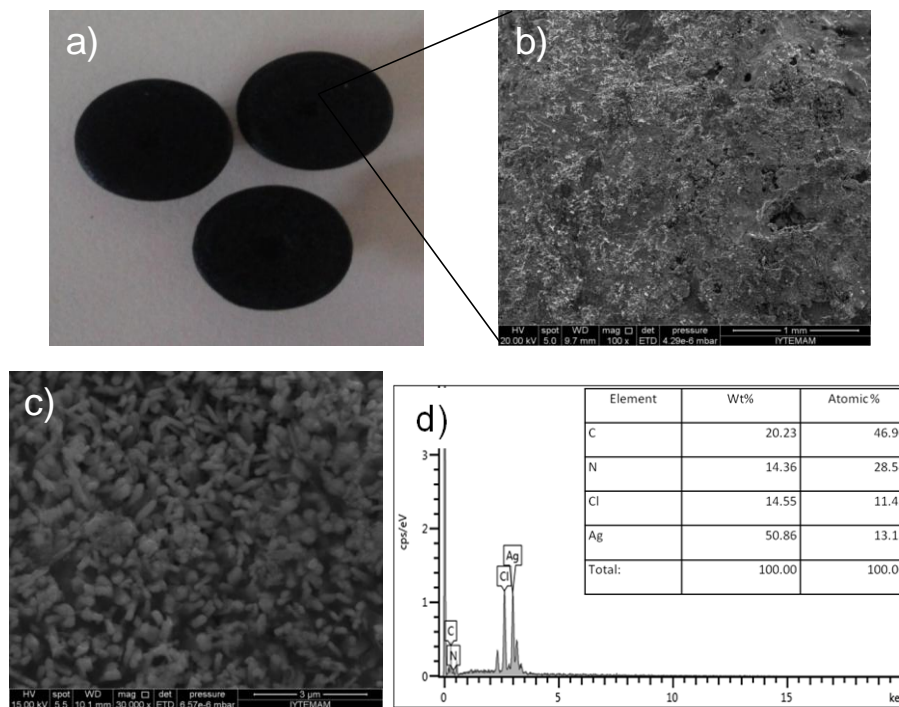
Figure 4.8. SEM images and EDS results of developed of ECG electrode with the new method.

Figure 4.9 shows SEM elemental mapping of the surface of ECG electrode developed by the new method. The image proves that homogenous distribution of Ag and Cl on the surface of electrode. Also, this mapping indicated the presence of N and C atoms on the coated surface. This means that the polyaniline is on the surface of ABS, besides the AgCl nanoparticles.
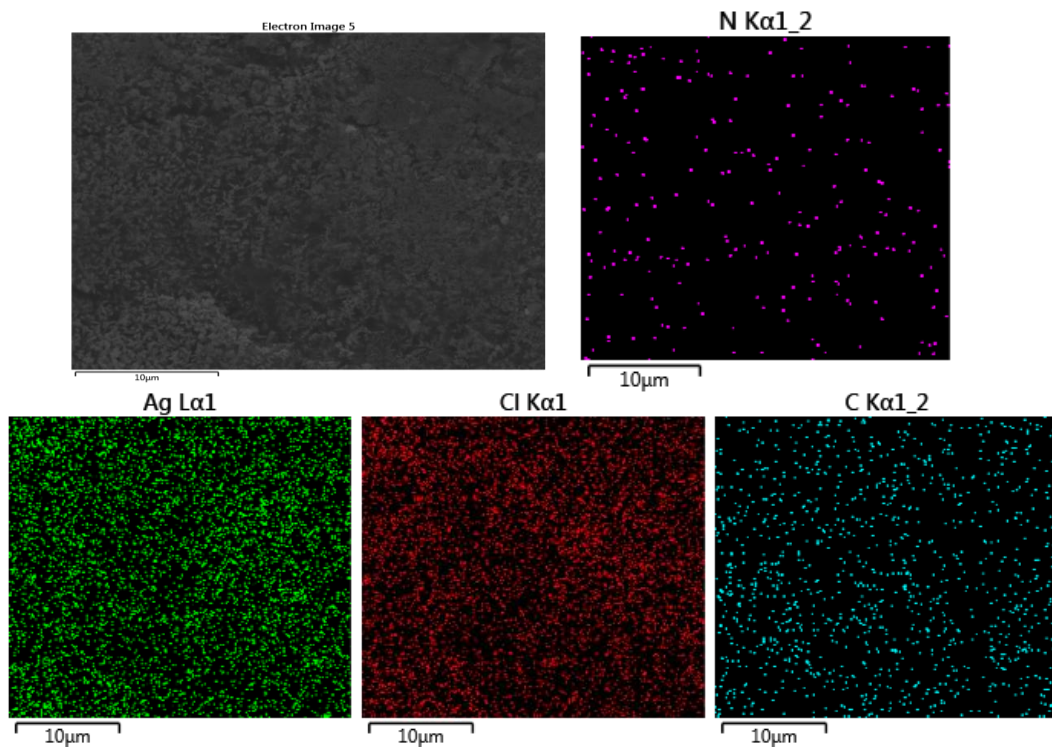
Figure 4.9. SEM elemental mapping of ECG electrode developed by the new method.

The picture and SEM image of a commercial Ag/AgCl ECG electrode were depicted in Figure 4.10. In Figure 4.10.b, demonstrates a rough surface of the electrode that might cause signal loss. Also, the SEM elemental mapping of the commercial Ag/AgCl ECG electrode indicates the uneven distribution of Ag and Cl on the electrode surface (Figure 4.11).
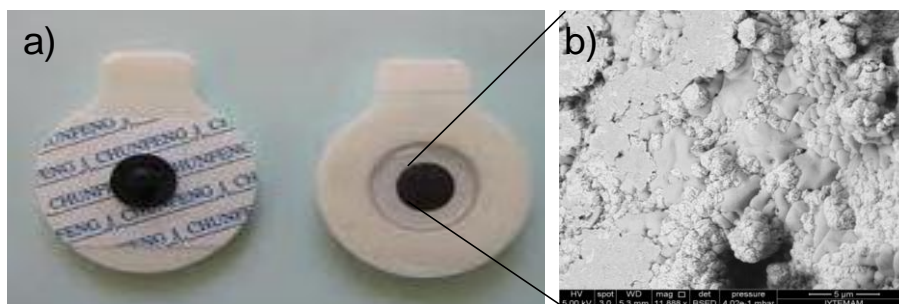
Figure 4.10. Picture and SEM image of a commercial ECG electrode
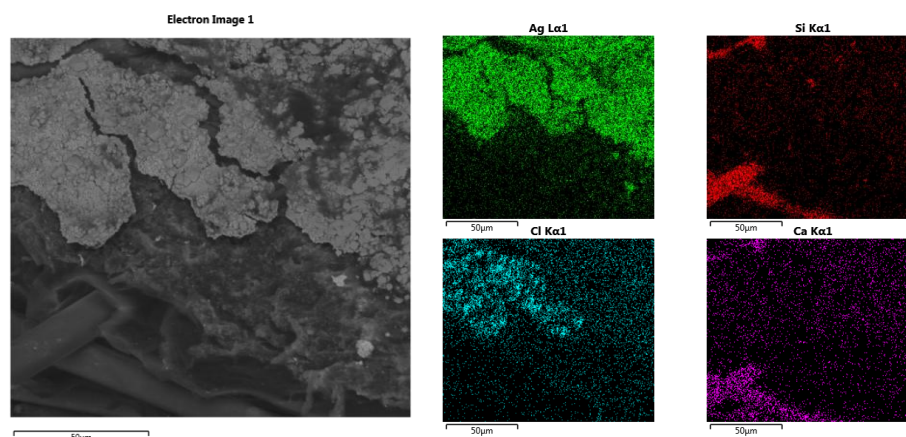
Element	Wt%	Atomic %
O	8.63	35.84
Si	0.45	1.07
Se	5.18	4.36
Ag	81.07	49.96
Cl	4.68	8.77
Total:	100.00	100.00

Figure 4.11. SEM picture of the commercial electrode and its elemental composition by SEM-EDS

4.3.1. Evalution of ECG electrodes

To evaluate the electrode performance, ECG measurement were conducted by using the electrodes with various coatings. The amount of $AgNO_3$ was changed during the fabrication of the electrode. Table 4.5. tabulates the concentration of $AgNO_3$ used during the coating process. When the concentration of $AgNO_3$ was 0.1 M to form Ag nanoparticles, the ECG signal was observed because the amount of AgCl nanoparticles on the surface of electrode was enough to convert ionic current to electron current (an electrical signal). However, when the concentration of $AgNO_3$ was decreased under 0.1 M to reduce the cost of ECG fabrication, the signals were not read because an amount of AgCl nanoparticles embedded in the PANI. Therefore, a new procedure was applied to decrease $AgNO_3$ amount (in case 5). Firstly, aniline polymerization was made on the surface of ABS. The polymerization process was 20 min. In the second step, this functionalized ABS surface was coated with composite layer (PANI and AgCl nanoparticles). However, the coating time was decreased from 20 minutes to 10 minutes

so as to form thin composite layer on the ABS surface. Also, contrary to the standart procedure of the fabricated of PANI and AgCl nanoparticle composite, the concentration of silver nitrate was reduced by half. Even if, the silver nitrate amount was reduced by half, the better results were obtained from ECG measurements. Since AgCl nanoparticles were on the top surface of the ABS depending on decreasing the coating thickness of PANI and AgCl nanoparticles composite.

Table 4.5. ECG measurements with different surface coatings.

Case	Coating variables	ECG measurement
1	Electrodes did not include AgCl NP	No signal
2	PANI with AgCl nanoparticles synthesized in the presence of 0.001 M AgNO$_3$	No signal
3	PANI with AgCl nanoparticles synthesized in the presence of 0.05 M AgNO$_3$	No signal
4	PANI with AgCl nanoparticles synthesized in the presence of 0.1 M AgNO$_3$	Signal was read
5	1) Only thin layer of PANI coating 2) PANI with AgCl nanoparticles synthesized in the presence of 0.05 M AgNO$_3$	Signal was read

After fabrication of the new ECG electrodes, these electrodes were compared with the commercial ECG electrodes. The fabricated new electrodes with AgCl nanoparticles by using 0.1 M AgNO$_3$ (procedure 4 in Table 4.5) were evaluated on the two different people. ECG measurements were made with the electrodes fabricated the procedure 4. The rhythm analysis of two different motienless patients was determined in Figure 4.12 and Figure 4.13. The rhythm analysis of these motienless patients shows that the signal to noise ratio of the electrodes was better than the commercial ones. The noise level was lower than one unit in the ECG graphs and the signal to noise ratio was approximately 50:1 for electrodes by procedure 4. When we compared the cardiac stress test (effort test) with commercial electrode for these two people in Figure 4.14 and

Figure 4.15, the noise level slightly increased but the signal to noise ratio (S/N) did not interfere with the right information on the ECG measurements, because S/N was 15:1 and this ratio was enough to obtain right information. However, the cost of these electrodes which were fabricated by procedure 4 was high. Therefore, we designed a new procedure for decreasing the fabrication cost and noise level.

PATIENT A-CARDIAC TEST

Figure 4.12. Comparative ECG signals observed from the commercial and the new electrodes for cardiac test in motionless patient (Patient A). This new electrode was in the case-4.

PATIENT B- CARDIAC TEST

Figure 4.13. Comparative ECG signals observed from the commercial and the new electrode for cardiac test in motionless patient (Patient B). This new electrode was in the case-4.

PATIENT A-CARDIAC STRESS TEST

Figure 4.14. Comparative ECG signals observed from the commercial and the new electrode for cardiac stress test (Patient A). This new electrode was in the case-4.

PATIENT B-CARDIAC STRESS TEST

Figure 4.15. Comparative ECG signals observed from the commercial and the new electrode for cardiac stress test (Patient B). This new electrode was in the case-4.

Fabricated the electrodes by using the procedure 5 (Table 4.5) were compared with the commercial electrodes and the fabricated electrodes with the procedure 4. Figure 4.16 indicates ECG map of commercial electrode and procedure 4 and procedure 5 for motionless patient B. The ECG measurements were compared with each other, the results were almost the same and S/N was very low. The effort tests of these three different ECG electrodes were in Figure 4.17. However, the fabricated ECG electrodes by using procedure 5 were better than the others. Because the noise level of the electrodes is low. These electrodes are inexpensive than the others.

PATIENT B-CARDIAC TEST WITH THREE DIFFERENT ELECTRODES

Figure 4.16. Comparative ECG signals observed from the commercial and the new electrodes for cardiac test.

PATIENT B-CARDIAC STRESS TEST WITH THREE DIFFERENT ELECTRODES
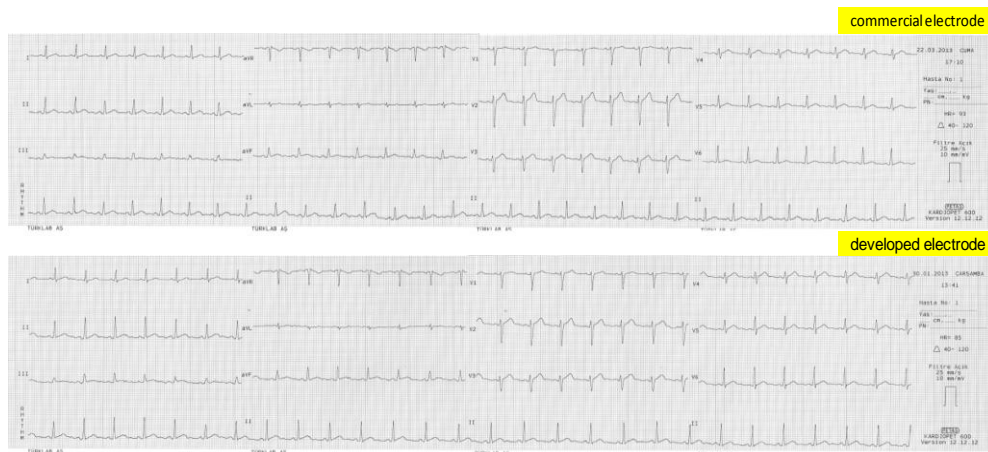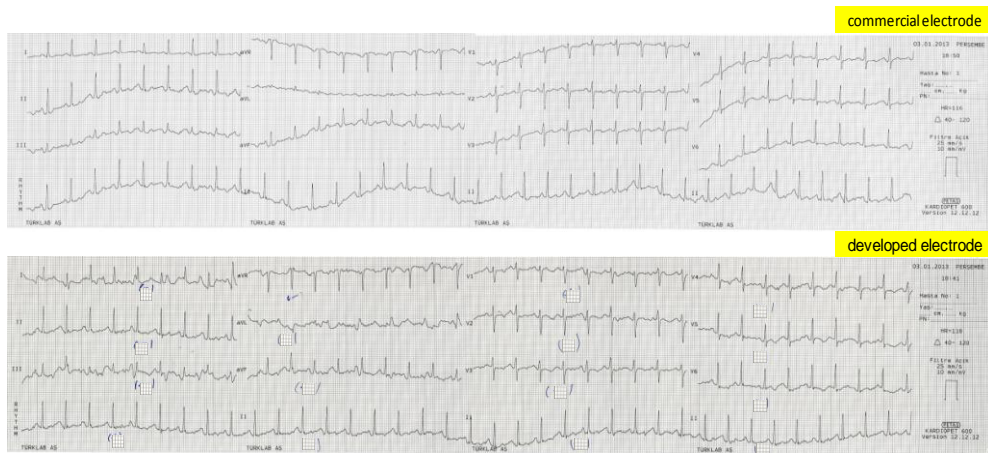

Figure 4.17. Comparative ECG signals observed from the commercial and the new electrodes for cardiac stress test.

The ECG measurements of commercial and new ECG electrodes which were fabricated with procedure 4 and procedure 5 were evaluated. There is no problem on the sizes and the widths of watched waves in three electrodes. Isoelectric line of these electrodes followed a straight. The noise or artifact was almost never observed in motionless patients for these electrodes. The noise level in effort test was very low to not alter the ECG measurement results. However, the fabrication cost of electrodes by procedure 5 was lower than the others.

4.4. Discussion

Contrary to used ECG electrodes at the present time, new ECG electrodes were developed. These ECG electrodes were fabricated by coating supporting material (ABS) with PANI and AgCl nanoparticles composite. In this study, we used aniline for very important two missions. Aniline is the monomer of polyaniline in this study. It is used as a reductant due to properties of weak reducing agent (Javed Ijaz Hussain 2011). Thus AgCl nanoparticles were synthesized with a different method in the literature. Wankhede and coworkers synthesized silver nanoparticles embedded in PANI in the similar studies (Y. B. Wankhede 2013a). They reported that the metal nanoparticles could be synthesized during the polymerization. They used nitric acid to provide acidic medium for polymerization. Unlike the study of Wankhede et al., we used HCl because of acidic medium for started polymerization and providing Cl^- source to form AgCl nanoparticles. When we tested these ECG electrodes on the human body and compared with the commercial electrodes, the electrodes which were fabricated with procedure 5 gave a best result. Since AgCl nanoparticles were on the top surface of the electrode. Thus, the ionic signals from the human body were detected in a better way and the ionic current converted to electron current in order to obtain electrical signal. If we compare new type ECG electrodes with commercial ones for normal cardiac test, our results are better than the commercial ones. Because the noise level of new electrodes was very low. However, for the cardiac stress test, our electrodes showed the similar results as the commercial electrodes. If the ECG electrodes are fabricated by coating ABS surface with only PANI without AgCl nanoparticles, the signals are not read. Since only PANI is not enough to convert ionic current to electron current.

4.5. Conclusion

We demonstrated that the ECG electrode was successfully fabricated by using PANI/AgCl nanoparticle composite. The surface of the ABS (Acrylonitrile Butadiene Styrene) which is the supporting material of ECG sensor was coated with AgCl nanoparticles by using a conductive linker (PANI). Simultaneous synthesis of AgCl nanoparticles and polymerization of aniline on the surface of ABS was achieved. The presence of AgCl nanoparticles on the ECG surface is required to relay the ionic signal generated in the body. Since a lower impedance to increase the signal to noise ratio is important. We used AgCl nanoparticles to fullfil this requirement. We proved the presence of AgCl nanoparticles doped in the ECG electrodes made PANI coating. We did not determine any signal from the body with the PANI ''only'' electrodes. Consequently, we developed a new method to fabricate ECG electrodes. The fabricated ECG electrodes in this thesis worked well. We propose that these electrodes can be a valuable product commercially because the fabrication of these electrodes is easy and inexpensive.

CHAPTER 5

CONCLUSION

The aim of this study is to develop a novel sensor consisting of silver chloride nanoparticles for ECG electrodes. In this study, firstly, Ag nanoparticles were synthesized in a wide range of sizes and at the different shapes like spherical, cube and wire before to synthesize AgCl nanoparticles. Then, the effect of molarity of silver source, molarity of Cl$^-$ source and the effect of reaction temperature in the polyol method were studied to obtain mono-sized and mono-shaped AgCl nanoparticles. As a result of this study, when the concentration of AgNO$_3$ was increased from 0.012 M to 0.094 M, the exciton band belongs to AgCl nanoparticles was shifted to higher wavelength depending on the size effect. Also, the reaction temperature was increased, the size of particles was increased. Ag nanoparticles were reformed on the surface of AgCl particles due to enhanced reducing ability of ethylene glycol at higher temperature. The concentration of HCl affects the formation and shape of the final product. The optimum conditions for 100 nm AgCl nanocubes were determined as 0.047 M silver nitrate, 0.0375 M PVP and 0.12 M HCl at 100 ºC.

Unfortunately, these AgCl nanoparticles did not directly adsorbed on the surface of ABS. Therefore, an additional material was needed for the adsorbtion of AgCl nanoparticles to the ABS surface. Conductive PANI was selected as a linker because it is conductive polymer and aniline polymerization on the ABS surface is easy. Nevertheless, synthesized AgCl nanoparticles which were added during polymerization were almost never adsorbed on the surface of ABS. Consequently, we did not read any ECG signals due to the lower amount of AgCl nanoparticles. For this reason, we performed to simultaneous aniline polymerization and synthesis of AgCl nanoparticles formation on the ABS surface. This method was worked out, thus a new ECG electrode was successfully developed based on PANI/AgCl nanoparticles. ECG signals were achieved by the new electrode. As a result, we suggest that this novel electrode can be fabricated with a low manufacturing cost.

REFERENCES

Abbasi, A. R., M. Bohloulzadeh, and A. Morsali. 2011. "Preparation of AgCl Nanoparticles@Ancient Textile with Antibacterial Activity under Ultrasound Irradiation." *Journal of Inorganic and Organometallic Polymers and Materials* no. 21 (3):504-510.

Ali Mansoori, G. 2005. *Principles Of Nanotechnology: Molecular-Based Study Of Condensed Matter In Small Systems*: World Scientific Pub Co Inc.

An, C. H., S. N. Peng, and Y. G. Sun. 2010. "Facile Synthesis of Sunlight-Driven AgCl:Ag Plasmonic Nanophotocatalyst." *Advanced Materials* no. 22 (23):2570-2574.

Anna Zielińska-Jurek, Joanna Reszczyńska, Ewelina Grabowska and Adriana Zaleska2012. "Nanoparticles Preparation Using Microemulsion Systems." In *Microemulsions - An Introduction to Properties and Applications* edited by Reza Najjar, 229-250. Poland: InTech.

Belloni, Jacqueline. 2003. "Photography: enhancing sensitivity by silver-halide crystal doping." *Radiation Physics and Chemistry* no. 67:291-296.

Blackman, John A. 2008. *Handbook of Metal Physics*. Edited by Prasanta Misra. 1 ed. Vol. 5, *Metallic Nanoparticles*: Elsevier Science.

Bonnemann, H., and R. M. Richards. 2001. "Nanoscopic metal particles - Synthetic methods and potential applications." *European Journal of Inorganic Chemistry* (10):2455-2480.

Cao, A., R. Lu, and G. Veser. 2010. "Stabilizing metal nanoparticles for heterogeneous catalysis." *Physical Chemistry Chemical Physics* no. 12 (41):13499-13510.

Carotenuto, G., G. P. Pepe, and L. Nicolais. 2000. "Preparation and characterization of nano-sized Ag/PVP composites for optical applications." *European Physical Journal B* no. 16 (1):11-17.

Choi, M., K. H. Shin, and J. Jang. 2010. "Plasmonic photocatalytic system using silver chloride/silver nanostructures under visible light." *Journal of Colloid and Interface Science* no. 341 (1):83-87.

Collier, C. P., R. J. Saykally, J. J. Shiang, S. E. Henrichs, and J. R. Heath. 1997. "Reversible tuning of silver quantum dot monolayers through the metal-insulator transition." *Science* no. 277 (5334):1978-1981.

Coskun, S., B. Aksoy, and H. E. Unalan. 2011. "Polyol Synthesis of Silver Nanowires: An Extensive Parametric Study." *Crystal Growth & Design* no. 11 (11):4963-4969.

Cushing, B. L., V. L. Kolesnichenko, and C. J. O'Connor. 2004. "Recent advances in the liquid-phase syntheses of inorganic nanoparticles." *Chemical Reviews* no. 104 (9):3893-3946.

Dekker, Markel. 2004. Preparation of polymer-capped metal nanoparticle by alcohol reduction. In *Dekker Encyclopedia of Nanoscience and Nanotechnology*. New York.

Dong, X. Y., X. H. Ji, J. Jing, M. Y. Li, J. Li, and W. S. Yang. 2010. "Synthesis of Triangular Silver Nanoprisms by Stepwise Reduction of Sodium Borohydride and Trisodium Citrate." *Journal of Physical Chemistry C* no. 114 (5):2070-2074.

Doria, G., J. Conde, B. Veigas, L. Giestas, C. Almeida, M. Assuncao, J. Rosa, and P. V. Baptista. 2012. "Noble Metal Nanoparticles for Biosensing Applications." *Sensors* no. 12 (2):1657-1687.

Ducampsanguesa, C., R. Herreraurbina, and M. Figlarz. 1992. "Synthesis and Characterization of Fine and Monodisperse Silver Particles of Uniform Shape." *Journal of Solid State Chemistry* no. 100 (2):272-280.

GHANI, MUHAMMAD FARID BIN AB. 2008. *Real-time ECG Acquisition System*, Faculty of Electronic and Computer Engineering, Universiti Teknikal Malaysia Melaka Malaysia.

Glaus, S., and G. Calzaferri. 2003. "The band structures of the silver halides AgF, AgCl, and AgBr: A comparative study." *Photochemical & Photobiological Sciences* no. 2 (4):398-401.

Han, L., P. Wang, C. Z. Zhu, Y. M. Zhai, and S. J. Dong. 2011. "Facile solvothermal synthesis of cube-like Ag@AgCl: a highly efficient visible light photocatalyst." *Nanoscale* no. 3 (7):2931-2935.

Herron, N., and D. L. Thorn. 1998. "Nanoparticles: Uses and relationships to molecular cluster compounds." *Advanced Materials* no. 10 (15):1173-+.

Huang, C. J., Y. H. Wang, P. H. Chiu, M. C. Shih, and T. H. Meen. 2006. "Electrochemical synthesis of gold nanocubes." *Materials Letters* no. 60 (15):1896-1900.

Jain, P. K., K. S. Lee, I. H. El-Sayed, and M. A. El-Sayed. 2006. "Calculated absorption and scattering properties of gold nanoparticles of different size, shape, and composition: Applications in biological imaging and biomedicine." *Journal of Physical Chemistry B* no. 110 (14):7238-7248.

Javed Ijaz Hussain[1], Sunil Kumar[2], Athar Adil Hashmi[1], Zaheer Khan[1,3*]. 2011. "Silver nanoparticles: preparation, characterization, and kinetics." *ADVANCED MATERIALS Letters* no. 2 (2):188-194.

Kang, S. Y., and K. Kim. 1998. "Comparative study of dodecanethiol-derivatized silver nanoparticles prepared in one-phase and two-phase systems." *Langmuir* no. 14 (1):226-230.

Katz, E., and I. Willner. 2004. "Integrated nanoparticle-biomolecule hybrid systems: Synthesis, properties, and applications." *Angewandte Chemie-International Edition* no. 43 (45):6042-6108.

Khan, M. A. M., S. Kumar, M. Ahamed, S. A. Alrokayan, and M. S. AlSalhi. 2011. "Structural and thermal studies of silver nanoparticles and electrical transport study of their thin films." *Nanoscale Research Letters* no. 6.

Khandpur, R. 2005. *Biomedical Instrumentation: Technology and Applications*: McGraw-Hill Education.

Kim, Chang Woo Kim ; Hyun Gil Cha ; Yong Chul Kang ; Young Soo Kang; Young Hwan. 2006. Preparation and characterization of Ag nanoparticle using hydrothermal process. In *Nanotechnology Materials and Devices Conference*.

Kim, S., H. Chung, J. H. Kwon, H. G. Yoon, and W. Kim. 2010. "Facile Synthesis of Silver Chloride Nanocubes and Their Derivatives." *Bulletin of the Korean Chemical Society* no. 31 (10):2918-2922.

Lee, K. S., and M. A. El-Sayed. 2006. "Gold and silver nanoparticles in sensing and imaging: Sensitivity of plasmon response to size, shape, and metal composition." *Journal of Physical Chemistry B* no. 110 (39):19220-19225.

Li, F., X. Q. Liu, Y. L. Yuan, J. F. Wu, and Z. Li. 2010. "Controllable synthesis, characterization and optical properties of Ag@AgCl coaxial core-shell nanocables." *Crystal Research and Technology* no. 45 (11):1189-1193.

L., J. Sun, X. R. Li, Y. Zhang, Z. X. Wang, C. R. Wang, J. W. Dai, and Q. B. Wang. 2012. "Controllable synthesis of monodispersed silver nanoparticles as standards for quantitative assessment of their cytotoxicity." *Biomaterials* no. 33 (6):1714-1721.

Liu, X. O., M. Atwater, J. H. Wang, and Q. Huo. 2007. "Extinction coefficient of gold nanoparticles with different sizes and different capping ligands." *Colloids and Surfaces B-Biointerfaces* no. 58 (1):3-7.

M. Brust , J. Fink , D. Bethell , D. J. Schiffrin and C. Kiely. 1995. "Synthesis and reactions of functionalised gold nanoparticles." *J. Chem. Soc., Chem. Commun.,*:1655-1656.

M. Brust, M. Walker, D. Bethell, D. J. Schiffrin and R. Whyman. 1994. "Synthesis of Thiol-derivatised Gold Nanoparticles in a Two-phase Liquid-Liquid System." *J. Chem. Soc., Chem. Commun.,*:801-802.

Malina, D., A. Sobczak-Kupiec, Z. Wzorek, and Z. Kowalski. 2012. "Silver Nanoparticles Synthesis with Different Concentrations of

Polyvinylpyrrolidone." *Digest Journal of Nanomaterials and Biostructures* no. 7 (4):1527-1534.

Maribel G. Guzmán, Jean Dille, Stephan Godet 2009. "Synthesis of silver nanoparticles by chemical reduction method and their antibacterial activity " *International Journal of Chemical and Biological Engineering* no. 2 (3):104-111.

Martin, C. R. 1994. "Nanomaterials - a Membrane-Based Synthetic Approach." *Science* no. 266 (5193):1961-1966.

Mazur, M. 2004. "Electrochemically prepared silver nanoflakes and nanowires." *Electrochemistry Communications* no. 6 (4):400-403.

Murphy, C. J., and N. R. Jana. 2002. "Controlling the aspect ratio of inorganic nanorods and nanowires." *Advanced Materials* no. 14 (1):80-82.

Nepijko, S. A., D. Kutnyakhov, S. I. Protsenko, L. V. Odnodvorets, and G. Schonhense. 2011. "Sensor and microelectronic elements based on nanoscale granular systems." *Journal of Nanoparticle Research* no. 13 (12):6263-6281.

Neuman, Michael R . 2000. "Biopotential Electrodes." In *The Biomedical Engineering Handbook*, edited by Joseph D. Bronzino. Boca Raton: CRC Press LLC.

Neuman, Michael R. 2001a. "Biopotential Electrodes." In *Medical Instrumentation*, edited by John G. Webster, 189-240.

Neuman, Michael R. 2001b. "Biopotential Electrodes." In *In Medical Instrumentation*, edited by John G. Webster, 189-240.

Nguyen V. Nghia, *, Nguyen N. K. Truong[1], Nguyen M. Thong[2], Nguyen P. Hung[2]. 2002. "Synthesis of Nanowire-Shaped Silver by Polyol Process of Sodium Chloride." *International Journal of Materials and Chemistry* no. 2 (2):75-78.

Nikoobakht, B., and M. A. El-Sayed. 2003. "Preparation and growth mechanism of gold nanorods (NRs) using seed-mediated growth method." *Chemistry of Materials* no. 15 (10):1957-1962.

Pal, S., Y. K. Tak, and J. M. Song. 2007. "Does the antibacterial activity of silver nanoparticles depend on the shape of the nanoparticle? A study of the gram-negative bacterium Escherichia coli." *Applied and Environmental Microbiology* no. 73 (6):1712-1720.

Papp, S., R. Patakfalvi, and I. Dekany. 2007. "Formation and stabilization of noble metal nanoparticles." *Croatica Chemica Acta* no. 80 (3-4):493-502.

Patil, R., E. Matveeva, and V. Parkhutik. 2002. "Simple chemical polymerization method for deposition of conducting polyaniline on surface of acrylonitrile butadiene styrene." *Journal of Applied Polymer Science* no. 85 (9):1904-1910.

Peng, S., and Y. G. Sun. 2011. "Ripening of bimodally distributed AgCl nanoparticles." *Journal of Materials Chemistry* no. 21 (31):11644-11650.

Petit, C., P. Lixon, and M. P. Pileni. 1993. "In-Situ Synthesis of Silver Nanocluster in Aot Reverse Micelles." *Journal of Physical Chemistry* no. 97 (49):12974-12983.

Qian, H., C. Dong, J. Peng, X. Qiu, Y. Xu, and J. Ren. 2007. "High-quality and water-soluble near-infrared photolumineseent CdHgTe/CdS quantum dots prepared by adjusting size and composition." *Journal of Physical Chemistry C* no. 111 (45):16852-16857.

Rafique, M. Y., L. Q. Pan, Q. U. A. Javed, M. Z. Iqbal, and L. H. Yang. 2012. "Influence of $NaBH_4$ on the size, composition, and magnetic properties of $CoFe_2O_4$ nanoparticles synthesized by hydrothermal method." *Journal of Nanoparticle Research* no. 14 (10).

Ramsden, Jeremy J. 2009. *Applied Nanotechnology*: Elsevier Inc.

Rao, C. N. R., G. U. Kulkarni, P. J. Thomas, and P. P. Edwards. 2002. "Size-dependent chemistry: Properties of nanocrystals." *Chemistry-a European Journal* no. 8 (1):29-35.

Ravishankar Rai V, Jamuna Bai A. 2011. "Nanoparticles and their potential application as antimicrobials." *Science against microbial pathogens: communicating current research and technological advances* no. 1:197-209.

Robert Plonsey, Roger C. Barr. 2007. "Bioelectric Potentials." In *Bioelectricity A Quantitative Approach*, 45-70. Springer US.

Roselina, N. R. N., A. Azizan, and Z. Lockman. 2012. "Synthesis of Nickel Nanoparticles Via Non-Aqueous Polyol Method: Effect of Reaction Time." *Sains Malaysiana* no. 41 (8):1037-1042.

S. D. Solomon, * M. Bahadory, A. V. Jeyarajasingam, S. A. Rutkowsky,, and and C. Boritz. 2007. "Synthesis and Study of Silver Nanoparticles." *Journal of Chemical Education* no. 84 (2).

S. Y. Kang, K. Kim. 1998. "comparative study of dodecanthiol derivatized silver nanoparticles prepared in one phase and two phase system." *Langmuir* no. 14 (1):226-230.

Sanders, A. W., D. A. Routenberg, B. J. Wiley, Y. N. Xia, E. R. Dufresne, and M. A. Reed. 2006. "Observation of plasmon propagation, redirection, and fan-out in silver nanowires." *Nano Letters* no. 6 (8):1822-1826.

Schonenberger, C., B. M. I. vanderZande, L. G. J. Fokkink, M. Henny, C. Schmid, M. Kruger, A. Bachtold, R. Huber, H. Birk, and U. Staufer. 1997. "Template synthesis of nanowires in porous polycarbonate membranes: Electrochemistry and morphology." *Journal of Physical Chemistry B* no. 101 (28):5497-5505.

Schulman, T. P. Hoar & J. H. 1943. "Transparent Water-in-Oil Dispersions: the Oleopathic Hydro-Micelle." *Nature* no. 152:102-103.

Silvert, P. Y., R. HerreraUrbina, N. Duvauchelle, V. Vijayakrishnan, and K. T. Elhsissen. 1996. "Preparation of colloidal silver dispersions by the polyol process .1. Synthesis and characterization." *Journal of Materials Chemistry* no. 6 (4):573-577.

Sun, C. H., P. Chen, and S. Y. Zhou. 2007. "AgCl nanoparticle nanowires fabricated by template method." *Materials Letters* no. 61 (8-9):1645-1648.

Sun, Y. G., B. Gates, B. Mayers, and Y. N. Xia. 2002. "Crystalline silver nanowires by soft solution processing." *Nano Letters* no. 2 (2):165-168.

Sun, Y. G., and Y. N. Xia. 2002. "Shape-controlled synthesis of gold and silver nanoparticles." *Science* no. 298 (5601):2176-2179.

Sun, Y. G., Y. D. Yin, B. T. Mayers, T. Herricks, and Y. N. Xia. 2002. "Uniform silver nanowires synthesis by reducing AgNO3 with ethylene glycol in the presence of seeds and poly(vinyl pyrrolidone)." *Chemistry of Materials* no. 14 (11):4736-4745.

Taleb, A., C. Petit, and M. P. Pileni. 1997. "Synthesis of highly monodisperse silver nanoparticles from AOT reverse micelles: A way to 2D and 3D self-organization." *Chemistry of Materials* no. 9 (4):950-959.

Tang, X. L., M. Tsuji, M. Nishio, and P. Jiang. 2009. "Roles of Chloride Anions in the Shape Evolution of Anisotropic Silver Nanostructures in Poly(vinylpyrrolidone) (PVP)-Assisted Polyol Process." *Bulletin of the Chemical Society of Japan* no. 82 (10):1304-1312.

Tao, A. R., S. Habas, and P. D. Yang. 2008. "Shape control of colloidal metal nanocrystals." *Small* no. 4 (3):310-325.

Thi My Dung Dang[1,] Thi Tuyet Thu Le[1,] Eric Fribourg-Blanc[2] and Mau Chien Dang[1]. 2011. "Synthesis and optical properties of copper nanoparticles prepared by a chemical reduction method." *Adv. Nat. Sci.: Nanosci. Nanotechnol.* no. 2.

Tran, T. N. D., N. Q. Buu, D. V. Quang, H. T. Ha, L. A. Bang, N. H. Chau, N. T. Ly, and N. V. Trung. 2009. "Synthesis of nanosilver particles by reverse micelle method and study of their bactericidal properties." *Apctp-Asean Workshop on Advanced Materials Science and Nanotechnology (Amsn08)* no. 187.

Turkevich, J.; Stevenson, P. C.; Hillier, J. 1951. "Nucleation and Growth Process in the Synthesis of Colloidal Gold." *Discuss. Faraday Soc.* no. 11:55-75.

Vasileva, P., B. Donkova, I. Karadjova, and C. Dushkin. 2011. "Synthesis of starch-stabilized silver nanoparticles and their application as a surface plasmon resonance-based sensor of hydrogen peroxide." *Colloids and Surfaces a-Physicochemical and Engineering Aspects* no. 382 (1-3):203-210.

Wan, Y., Z. Guo, X. Jiang, K. Fang, X. Lu, Y. Zhang, and N. Gu. 2013. "Quasi-spherical silver nanoparticles: aqueous synthesis and size control by the seed-mediated Lee-Meisel method." *J Colloid Interface Sci* no. 394:263-8.

Wang, H. S., X. L. Qiao, J. G. Chen, X. J. Wang, and S. Y. Ding. 2005. "Mechanisms of PVP in the preparation of silver nanoparticles." *Materials Chemistry and Physics* no. 94 (2-3):449-453.

Wiley, B., T. Herricks, Y. G. Sun, and Y. N. Xia. 2004a. "Polyol synthesis of silver nanoparticles: Use of chloride and oxygen to promote the formation of single-crystal, truncated cubes and tetrahedrons." *Nano Letters* no. 4 (9):1733-1739.

Wiley, B., T. Herricks, Y. G. Sun, and Y. N. Xia. 2004b. "Polyol synthesis of silver nanoparticles: Use of chloride and oxygen to promote the formation of single-crystal, truncated cubes and tetrahedrons (vol 4, pg 1734, 2004)." *Nano Letters* no. 4 (10):2057-2057.

Wiley, B. J., Y. C. Chen, J. M. McLellan, Y. J. Xiong, Z. Y. Li, D. Ginger, and Y. N. Xia. 2007. "Synthesis and optical properties of silver nanobars and nanorice." *Nano Letters* no. 7 (4):1032-1036.

Wiley, B., Y. G. Sun, B. Mayers, and Y. N. Xia. 2005. "Shape-controlled synthesis of metal nanostructures: The case of silver." *Chemistry-a European Journal* no. 11 (2):454-463.

Xu, H. X., and K. S. Suslick. 2010. "Sonochemical Synthesis of Highly Fluorescent Ag Nanoclusters." *Acs Nano* no. 4 (6):3209-3214.

Y. B. Wankhede[1,] S. B. Kondawar[2, *], S. R. Thakare[3], P. S. More[4]. 2013a. "Synthesis and characterization of silver nanoparticles embedded in polyaniline nanocomposite." *Adv. Mat. Lett.* no. 4 (1):89-93

Y. B. Wankhede[1,] S. B. Kondawar[2,] S. R. Thakare[3], P. S. More[4]. 2013b. "Synthesis and characterization of silver nanoparticles embedded in polyaniline nanocomposite." *Advanced Materials Letters* no. 4 (1):89-93.

Yang, X. G., S. H. Chen, S. Y. Zhao, D. G. Li, and H. Y. Ma. 2003. "Synthesis of copper nanorods using electrochemical methods." *Journal of the Serbian Chemical Society* no. 68 (11):843-847.

Yazicioglu, Refet Firat, Hoof, Chris van, Puers, Robert. 2009. "Introduction to Biopotential Acquisition." In *biopotential readout circuits for portable acquisition systems*. Springer Science + Business Media B.V.

Yi, Z., X. B. Xu, X. Q. Wu, C. H. Chen, X. B. Li, B. C. Luo, J. S. Luo, X. D. Jiang, W. D. Wu, Y. G. Yi, and Y. J. Tang. 2013. "Silver nanoplates: controlled preparation, self-assembly, and applications in surface-enhanced Raman scattering." *Applied Physics a-Materials Science & Processing* no. 110 (2):335-342.

Zhu, J. J., C. X. Kan, J. G. Wan, M. Han, and G. H. Wang. 2011. "High-Yield Synthesis of Uniform Ag Nanowires with High Aspect Ratios by Introducing the Long-Chain PVP in an Improved Polyol Process." *Journal of Nanomaterials*.

Zhu, M. S., P. L. Chen, and M. H. Liu. 2011. "Graphene Oxide Enwrapped Ag/AgX (X = Br, Cl) Nanocomposite as a Highly Efficient Visible-Light Plasmonic Photocatalyst." *Acs Nano* no. 5 (6):4529-4536.

Zhu, M. S., P. L. Chen, and M. H. Liu. 2012. "Ag/AgBr/Graphene Oxide Nanocomposite Synthesized via Oil/Water and Water/Oil Microemulsions: A Comparison of Sunlight Energized Plasmonic Photocatalytic Activity." *Langmuir* no. 28 (7):3385-3390.